Accepted Manuscript

Targeting the subpocket in xanthine oxidase: Design, synthesis, and biological evaluation of 2-[4-alkoxy-3-(1*H*-tetrazol-1-yl) phenyl]-6-oxo-1,6-dihydropyrimidine-5-carboxylic acid derivatives

Bing Zhang, Xiwen Dai, Ziyang Bao, Qing Mao, Yulin Duan, Yuwei Yang, Shaojie Wang

PII: S0223-5234(19)30683-X

DOI: https://doi.org/10.1016/j.ejmech.2019.07.062

Reference: EJMECH 11559

To appear in: *European Journal of Medicinal Chemistry*

Received Date: 5 June 2019

Revised Date: 14 July 2019

Accepted Date: 21 July 2019

Please cite this article as: B. Zhang, X. Dai, Z. Bao, Q. Mao, Y. Duan, Y. Yang, S. Wang, Targeting the subpocket in xanthine oxidase: Design, synthesis, and biological evaluation of 2-[4-alkoxy-3-(1*H*-tetrazol-1-yl) phenyl]-6-oxo-1,6-dihydropyrimidine-5-carboxylic acid derivatives, *European Journal of Medicinal Chemistry* (2019), doi: https://doi.org/10.1016/j.ejmech.2019.07.062.

1. Graphical Abstract

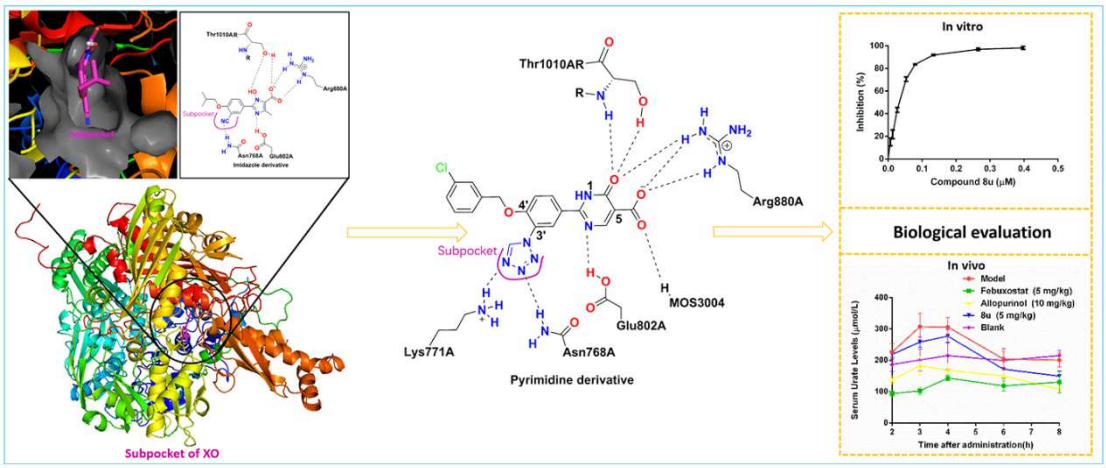

Targeting the subpocket in xanthine oxidase: design, synthesis, and biological evaluation of 2-[4-alkoxy-3-(1*H*-tetrazol-1-yl) phenyl]-6-oxo-1,6-dihydropyrimidine-5-carboxylic acid derivatives

Bing Zhang, Xiwen Dai, Ziyang Bao, Qing Mao, Yulin Duan, Yuwei Yang, Shaojie Wang*

Key Laboratory of Structure-Based Drugs Design & Discovery of Ministry of Education, School of Pharmaceutical Engineering, Shenyang Pharmaceutical University, 103 Culture Road, Shenhe District, Shenyang 110016, China

.

*Corresponding authors.

Tel/Fax: +86-24-43520230, E-mail: sjwang_99@163.com (S. J. Wang).

Abstract

Xanthine oxidase is an important target for the treatment of hyperuricemia, gout and other related diseases. Analysis of the high-resolution structure of xanthine oxidase with febuxostat identified the existence of a subpocket formed by the residues Leu648, Asn768, Lys771, Leu1014 and Pro1076. In this study, we designed and synthesized a series of 2-[4-alkoxy-3-(1*H*-tetrazol-1-yl) phenyl]-6-oxo-1,6-dihydropyrimidine-5-carboxylic acid derivatives (**8a**-**8z**) with a tetrazole group targeting this subpocket of the xanthine oxidase active site, and they were further evaluated for their inhibitory potency against xanthine oxidase *in vitro*. The results showed that all the tested compounds (**8a**-**8z**) exhibited an apparent xanthine oxidase inhibitory potency, with IC_{50} values ranging from 0.0288 μM to 0.629 μM. Among them, compound **8u** emerged as the most potent xanthine oxidase inhibitor, with an IC_{50} value of 0.0288 μM, which was comparable to febuxostat (IC_{50} = 0.0236 μM). The structure-activity relationship results revealed that the hydrophobic group at the 4′-position was indispensable for the inhibitory potency *in vitro* against xanthine oxidase. A Lineweaver-Burk plot revealed that the representative compound **8u** acted as a mixed-type inhibitor for xanthine oxidase. Furthermore, molecular modeling studies were performed to gain insights into the binding mode of **8u** with xanthine oxidase and suggested that the tetrazole group of the phenyl unit was accommodated in the subpocket, as expected. Moreover, a potassium oxonate-induced hyperuricemia model in rats was chosen to further confirm the hypouricemic effect of compound **8u**, and the result demonstrated that compound **8u** could effectively reduce serum uric acid levels at an oral dose of 5 mg/kg. In addition, acute oral toxicity study in mice indicated that compound **8u** was nontoxic and tolerated at a dose up to 2000 mg/kg. Thus, compound **8u** could be a potential and efficacious agent in treatment of hyperuricemia with low toxicity.

***Key words*:** 6-Oxo-1,6-dihydropyrimidine-5-carboxylic acid; Tetrazole; Xanthine oxidase inhibitor; Subpocket; Synthesis

1. Introduction

Xanthine oxidase (XO) is a molybdoenzyme catalyzing the oxidation of hypoxanthine to xanthine and xanthine to urate in the last two steps of purine nucleotide metabolism [1-3]. Uric acid is the final product of purine metabolism in humans, and the high level of uric acid in the plasma has been linked to a number of pathologies, such as gout, cardiovascular diseases, hypertension and renal diseases [4-6]. Therefore, XO is considered to be the most promising target for controlling the uric acid level and for the treatment of hyperuricemia, gout and other related diseases [7].

Allopurinol (**Fig. 1**), a prototype XO inhibitor and a hypoxanthine isomer, is a widely used drug for inhibiting XO in gout. However, in some cases, the interactions of purine analogs XO inhibitors on activities of purine and pyrimidine metabolizing enzymes lead to the reported hypersensitivity (Stevens-Johnsons) syndrome characterized by fever, skin rash, hepatitis, leukocytosis with eosinophilia and worsening renal function induced in some of the patients [8-10].

Therefore, finding the nonpurine compounds with potent XO-inhibition potency and fewer side effects than the purine analogs is in great demand. Considering these side effects, some nonpurine based XO inhibitors, such as febuxostat (approved in USA, 2009) [11], topiroxostat (approved in Japan, 2013) [12], Y-700 [13], isoxazole derivatives [14], selenazole derivatives [15], imidazole derivatives [16], 2-(indol-2-yl)-thiazole derivatives [17], 1,2,3-triazole derivatives [18], pyrazole derivatives [19], isonicotinic acid derivatives [20], 2-mercaptopyridine derivatives [21], isocytosine derivatives [22], pyrimidine derivatives [23], fused pyrano [3, 2-d] pyrimidine derivatives [24], dihydropyridazine derivatives [25], naphthopyran derivatives [26] and naphthoflavone derivatives [27] have been developed (**Fig. 1**). Additionally, other XO inhibitors with various chemotypes, including 4-pyridyl-1*H*-imidazole derivatives [28], 5-(4-pyridyl)-1,2,4-triazole derivatives [29], 2-benzylamino-4-methyl-1,3-thiazole derivatives [30], 5-[4-(pyridin-4-yl)-1*H*-1,2,3-triazol-1-yl] benzonitrile derivatives [31], *N*-(4-alkoxy-3-cyanophenyl) isonicotinamide/nicotinamide derivatives [32], 4,6-diaryl/heteroaryl pyrimidone derivatives [33] and pyrimidine-2,4-diamine derivatives [34], have also been published in the literature. However, febuxostat is no longer a precise and safe therapy for hyperuricemia because the FDA added a black-box warning to this drug due to its heart-related complications [35]. Therefore, there is still a need to explore new nonpurine XO inhibitors with fewer side effects for the treatment of hyperuricemia and gout.

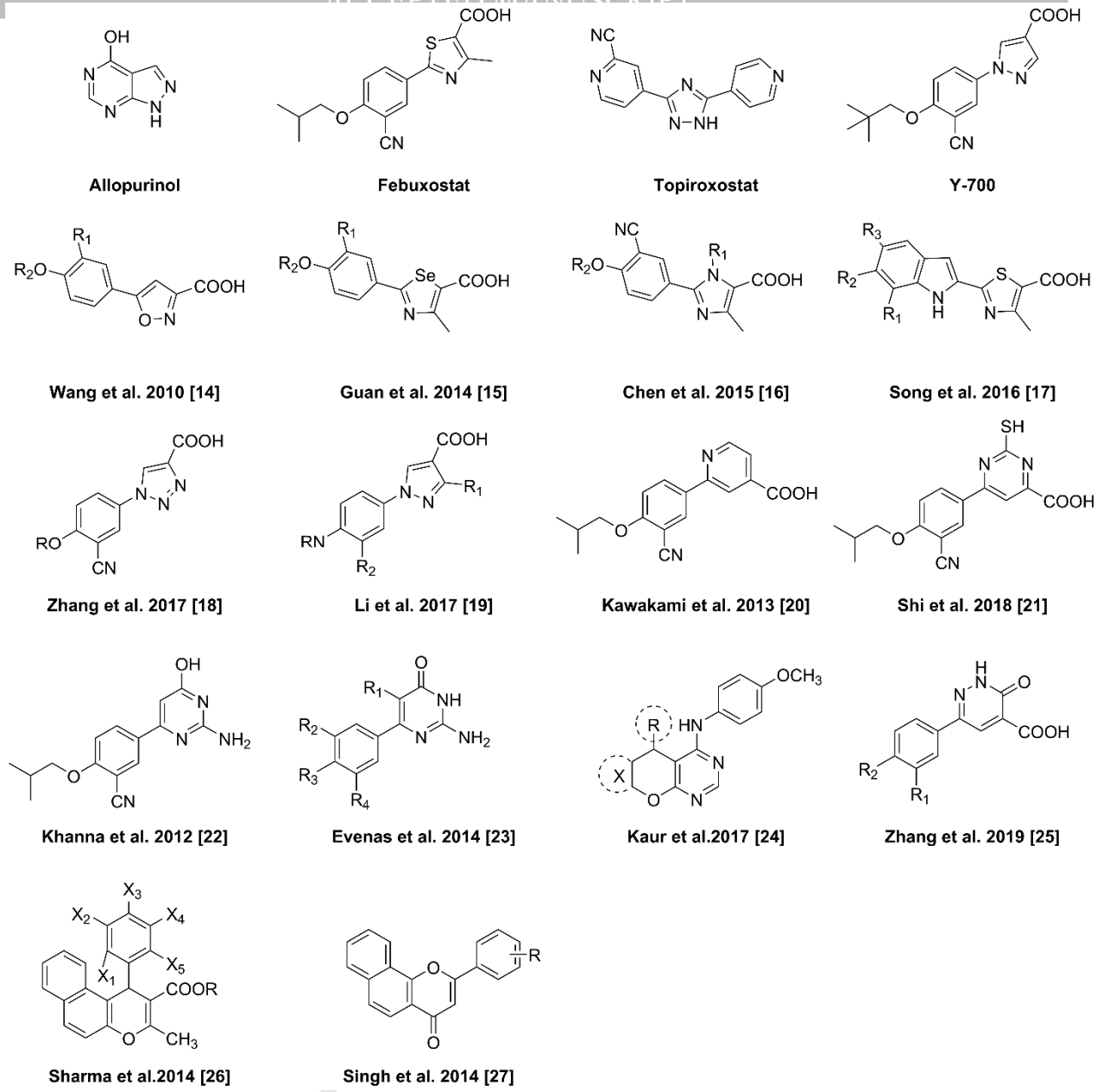

Fig. 1. Chemical structures of allopurinol and nonpurine XO inhibitors.

Analysis of the high-resolution structure (**Fig. 2a**) of XO with febuxostat could identify the existence of a subpocket formed by Leu648, Asn768, Lys771, Leu1014 and Pro1076 residues (**Fig. 2b**), and it was observed that the cyano group of febuxostat could interact with the Asn768 residue deep inside the subpocket (**Fig. 2c**). In many biologically important enzyme targets, targeting the unique subpocket of an enzyme active site could impart selectivity by modulators [36-40], which would help to further avoid some side effects [41-42]. As a consequence, the subpocket of the XO active site could be utilized for the development of the new nonpurine XO inhibitors with increased selectivity and fewer side effects. The tetrazole moiety is a low-toxic and practically nonmetabolized heterocyclic fragment acting as a hydrogen acceptor similar to the cyano group

[43-45], and the tetrazole moiety has received major attention from medicinal chemists due to its wide applications in the treatment of neonatal sepsis (latamoxef, approved in 1982) [46], hypertension (losartan, approved in 1994) [47] and symptoms of intermittent claudication (cilostazol, approved in 1988) [48]. Thus, the tetrazole moiety occupies an important position in the discovery of new drugs [49]. Therefore, we attempted to introduce a tetrazole moiety targeting the subpocket at the XO active site, with the hope of the tetrazole moiety filling the subpocket, which is useful for helping ligands anchored tightly to the binding site, enhancing the binding affinity [32, 50-52] and potentially preventing some side effects.

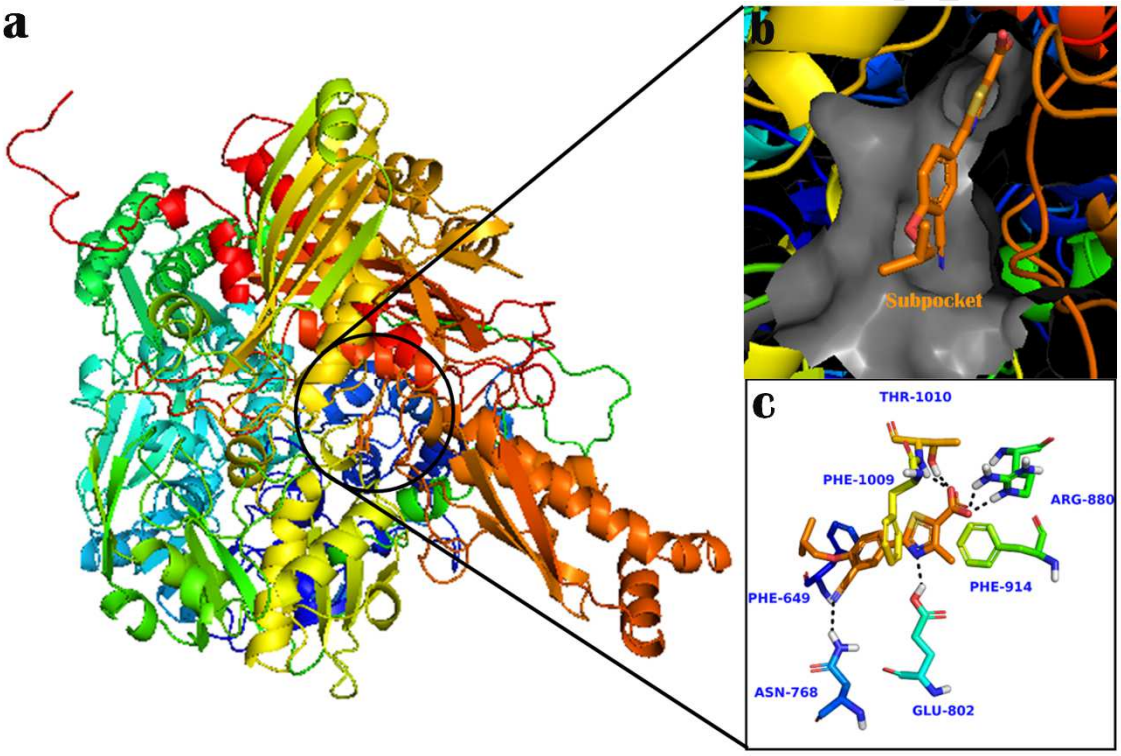

Fig. 2. Structure analysis of the XO-febuxostat complex. (a) Crystal structure of the XO-febuxostat complex as a cartoon representation. (b) The subpocket is shown as a gray surface and febuxostat is represented as an orange line. (c) Febuxostat is represented as an orange line, and key polar interactions are depicted with black dashed lines.

In our previous report, we explored several new classes of nonpurine XO inhibitors, including isoxazole derivatives [14], imidazole derivatives [16] and 4-pyridyl-1*H*-imidazole derivatives [28]. Among them, imidazole derivatives containing a 1-hydroxyimidazole moiety showed excellent inhibitory potency *in vitro* against XO [16], and structure-activity relationship analysis and molecular modeling studies indicated that the 1-hydroxy moiety could form an extra H-bond with Thr1010 and contribute to the inhibitory potency [16,28].

The results inspired us to further explore novel XO inhibitors based on an extra H-bond with Thr1010 in addition to the interactions between the carboxyl group and Arg880 and Thr1010. Pyrimidine, a six membered heterocyclic compound bearing two N-atoms in the ring, is usually used as an important pharmacophore for the design of many drugs, such as anticancer, antiviral and antibacterial agents [53], and there are also many successful examples of replacing five-membered heterocycles with the pyrimidine heterocycle in rational drug design [54]. In addition, several nonpurine XO inhibitors containing a pyrimidine heterocycle were also reported [21-24], so it was suggested that the pyrimidine group could be used as a potent pharmacophore to replace the imidazole ring of imidazole derivatives [16]. Accordingly, we attempted to adopt the pyrimidine ring to replace the imidazole ring by the bioisosteric replacement strategy and replace the cyano group with the tetrazole group to design a series of 2-[4-alkoxy-3-(1*H*-tetrazol-1-yl) phenyl]-6-oxo-1,6-dihydropyrimidine-5-carboxylic acid derivatives (**Fig**. **3**).

In this paper, we described the synthesis, *in vitro* bioevaluation and structure-activity relationships of 2-[4-alkoxy-3-(1*H*-tetrazol-1-yl) phenyl]-6-oxo-1,6-dihydropyrimidine-5-carboxylic acid derivatives (**8a**-**8z**) with a tetrazole group targeting the subpocket formed by Leu648, Asn768, Lys771, Leu1014 and Pro1076 residues in the XO active site. Moreover, we determined the inhibitory behavior of the representative compound **8u** by using molecular modeling studies, steady-state kinetic analysis and a hyperuricemic rat model, as well as its acute oral toxicity.

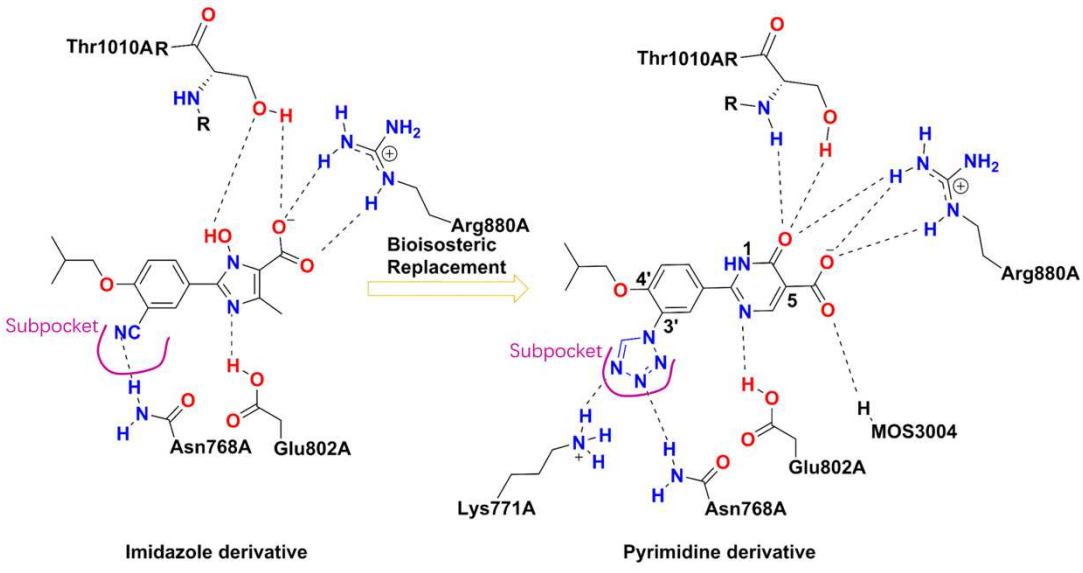

Fig. 3. Design strategy.

2. Results and discussion

2.1. Chemistry

The synthesis of the 2-[4-alkoxy-3-(1*H*-tetrazol-1-yl)phenyl]-6-oxo-1,6-dihydropyrimidine-5-carboxylic acids **8a-8y** and the 2-[4-hydroxy-3-(1*H*-tetrazol-1-yl) phenyl]-6-oxo-1, 6-dihydropyrimidine-5-carboxylic acid **8z** reported in this study are described in **Scheme 1**. The commercially available 4-hydroxybenzonitrile (**1**) was nitrated with nitric acid in acetic acid to provide 4-hydroxy-3-nitrobenzonitrile (**2**) at a good yield, which was then reduced under a hydrogen atmosphere catalyzed by Pd/C in methanol to obtain 3-amino-4-hydroxybenzonitrile (**3**) with high efficiency. Cyclization of the 3-amino-4-hydroxybenzonitrile (**3**) with triethyl orthoformate and sodium azide in acetic acid generated the key intermediate (**4**) [55] with a moderate yield, which was further alkylated with the appropriate alkyl halides in the presence of anhydrous potassium carbonate and potassium iodide in DMF to give excellent yields of 4-alkoxy-3-(1*H*-tetrazol-1-yl) benzonitriles **5a-5y**. The resulting intermediates **5a-5y** were treated with sodium methoxide and anhydrous methanol to afford the imidates, which following aminolysis with ammonium chloride, gave 4-alkoxy-3-(1*H*-tetrazol-1-yl) benzimidamide hydrochloride compounds **6a-6y** [56] in moderate yields. The condensation reaction of diethyl ethoxymethylenemalonate with 4-alkoxy-3-(1*H*-tetrazol-1-yl) benzimidamide hydrochloride compounds **6a-6y** in the presence of sodium ethoxide as an alkaline catalyst provided ethyl 2-[4-alkoxy-3-(1*H*-tetrazol-1-yl) phenyl]-6-oxo-1,6-dihydropyrimidine-5-carboxylates **7a-7y** [57] in good yields, and this reaction was followed by hydrolysis reactions using an aqueous solution of lithium hydroxide to give 2-[4-alkoxy-3-(1*H*-tetrazol-1-yl)phenyl]-6-oxo-1,6-dihydropyrimidine-5- carboxylic acids **8a-8y**.

The 2-[4-hydroxy-3-(1*H*-tetrazol-1-yl)phenyl]-6-oxo-1,6-dihydropyrimidine-5-carboxylic acid **8z** was obtained by removing the benzyl protecting group of the compound **8i** under a hydrogen atmosphere at room temperature catalyzed by Pd/C in DMF.

The structures were elucidated by HRMS, IR, ^{1}H NMR and ^{13}C NMR spectra. All spectral data were in accordance with the assumed structures. HRMS analysis revealed the target compounds with $[M-H]^-$ ion peaks. The IR spectra of the target compounds displayed hydroxyl stretching vibrations at 3402.8-3470.2 cm^{-1} (**8a-8y**) and a phenolic hydroxyl stretching vibration at 3561.9 cm^{-1} (**8z**). In ^{1}H NMR spectra, the CH of the tetrazole group was observed as a singlet at approximately 9.80 ppm in the series **8a-8z**.

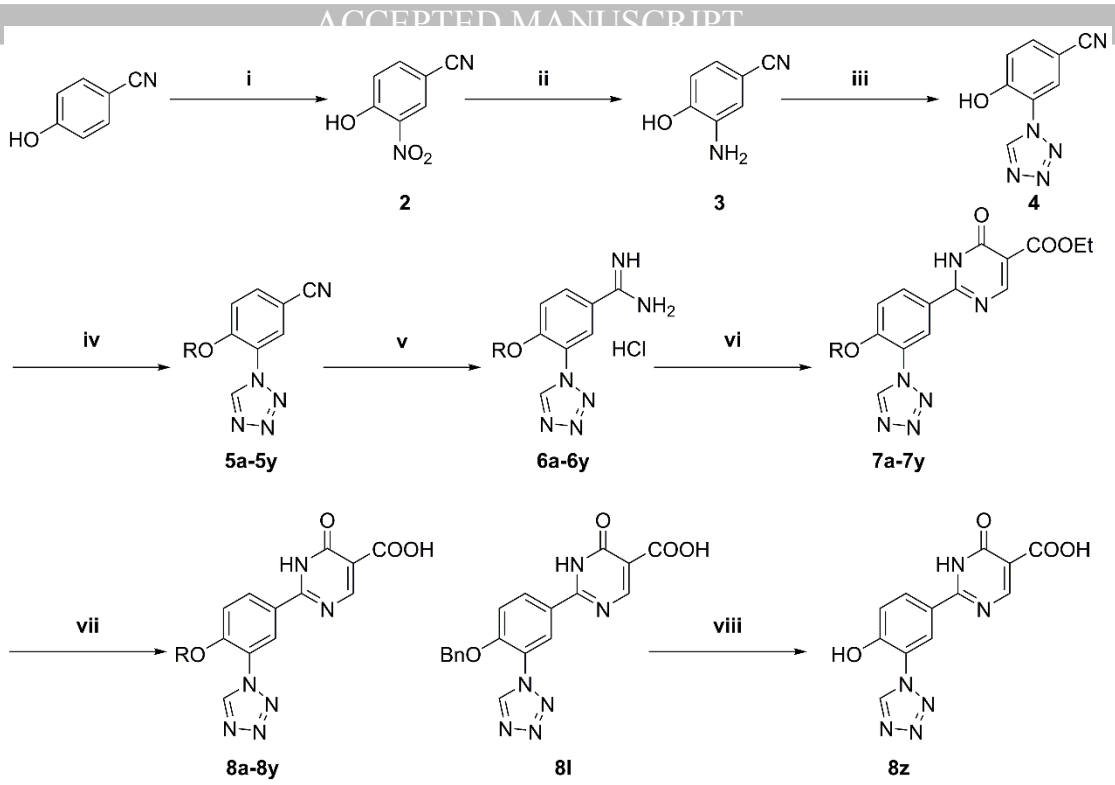

a : R = methyl
b : R = Isopropyl
c : R = Isobutyl
d : R = Isopropyl
e : R = allyl
f : R = 2-methylallyl
g : R = 3-methylbut-2-en-1-yl
h : R = prop-2-yn-1-yl
i : R = cyclopropylmeth
j : R = cyclopentyl
k : R = cyclohexylmeth
l : R = benzyl
m : R = 4-methylbenzyl
n : R = 4-(*tert*-butyl)benzyl
o : R = 4-methoxybenzyl
p : R = 4-fluorobenzyl
q : R = 4-chlorobenzyl
r : R = 4-bromobenzyl
s : R = 3-methoxybenzyl
t : R = 3-fluorobenzyl
u : R = 3-chlorobenzyl
v : R = 3-bromobenzyl
w : R = 2-chlorobenzyl
x : R = 2,6-dichlorobenzyl
y : R = 2,4-dichlorobenzyl
z : R = hydrogen

Scheme 1. Reagents and conditions: i. HNO_3, HAc, 75°C; ii. Pd/C, H_2, MeOH, 25°C; iii. NaN_3, triethyl orthoformate, HAc, 60°C; iv. R_1Cl or R_1Br, K_2CO_3, KI, DMF, 50-65°C; v. MeONa, MeOH, 25°C, 36 h, then NH_4Cl, 50°C; vi. diethyl ethoxymethylenemalonate, NaH, EtOH, 25°C; and vii. LiOH, H_2O, THF, 50°C.

2.2. Biological activity in vitro

The *in vitro* bovine XO inhibitory activity of compounds **8a-8z** was measured spectrophotometrically by determining uric acid production at 295 nm. Febuxostat and allopurinol were included as the positive controls. The testing results are shown in **Table 1**. All compounds exhibited excellent inhibitory potency with IC_{50} values ranging from 0.0288 μM to 0.629 μM. In particular, compound **8u** with a 3-chlorobenzyloxy group substituted at the 4′-position emerged as the most potent XO inhibitor (IC_{50} = 0.0288 μM), which was comparable to febuxostat (IC_{50} = 0.0236 μM) and had an IC_{50} value 264-fold higher than that of allopurinol (IC_{50} = 7.590 μM).

Table 1

In vitro XO inhibitory potency of designed compounds

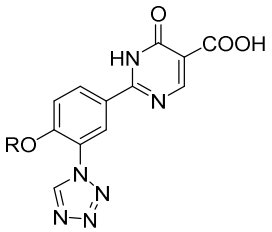

Compound	R	IC_{50} (μM)[a]	Compound	R	IC_{50} (μM)[a]
8a		0.0920±0.00428	**8o**	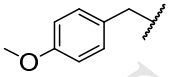	0.0507±0.00208
8b		0.0737±0.00172	**8p**	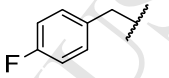	0.0531±0.00394
8c		0.0644±0.00279	**8q**	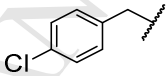	0.0691±0.00443
8d	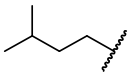	0.0541±0.00236	**8r**	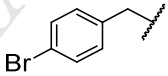	0.0552±0.00193
8e		0.0437±0.00105	**8s**	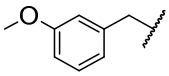	0.0516±0.00319
8f	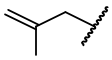	0.0569±0.000486	**8t**	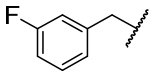	0.0477±0.00187
8g	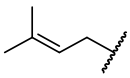	0.0692±0.00406	**8u**	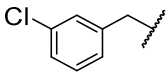	0.0288±0.00239
8h	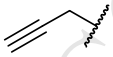	0.0500±0.00326	**8v**	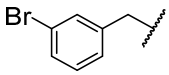	0.0450±0.00131
8i	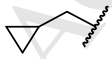	0.0461±0.00298	**8w**	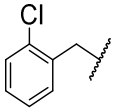	0.0917±0.00357
8j		0.0585±0.0000781	**8x**	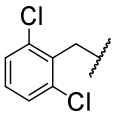	0.0639±0.00305
8k	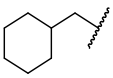	0.0683±0.00339	**8y**	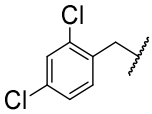	0.0838±0.00657

8l	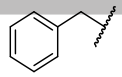	0.0945±0.00295	**8z**		0.629±0.0374
8m	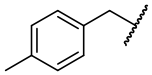	0.0894±0.00745	Febuxostat		0.0236±0.00230
8n	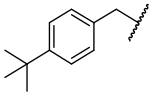	0.149±0.0160	Allopurinol		7.590±0.215

a. All values are expressed as the mean ± standard error of the mean of triplicate determinations.

Among the tested compounds, increasing the size of the substituent at the 4′-position of the phenyl moiety from a methoxy to an isopentyloxy group could steadily improve the XO inhibitory potency (**8a** < **8b** < **8c** < **8d**, IC_{50} = 0.0920 μM, 0.0737 μM, 0.0646 μM and 0.0541 μM, respectively). This finding indicated that increasing the size of saturated alkoxy groups at the 4′-position of the phenyl moiety could favor the XO inhibitory potency, which may be due to the improved hydrophobic interactions with nonpolar residues at the entrance of the pocket [22], and similar inhibitory behavior could also be observed for selenazole derivatives [15]. The replacement of a methoxy group with an allyloxy group at the 4′-position of the phenyl moiety led to approximately a 2-fold increase in the inhibitory potency (**8e** vs **8a**, IC_{50} = 0.0437 μM and 0.0920 μM, respectively), and when the methyl substituent was introduced into the double bond of the allyloxy group (**8e**), the inhibitory potency slightly decreased (**8e** > **8f** > **8g**, IC_{50} = 0.0437 μM, 0.0569 μM and 0.0692 μM, respectively). Meanwhile, a decrease in the inhibitory potency was also observed by increasing the size of cycloalkoxy groups, such as cyclopropylmethoxy, cyclopentyloxy and cyclohexylmethoxy groups (**8i** > **8j** > **8k**, IC_{50} = 0.0461 μM, 0.0585 μM and 0.0683 μM, respectively), implying that increasing the size of the olefinoxy groups or the cycloalkoxy groups at the 4′-position of the phenyl moiety could damage the XO inhibitory potency, which may be due to the steric hindrance of the substituents with the amino acids at the entrance of the active pocket. Moreover, the introduction of the propargyloxy group at the 4′-position did not translate into improvement in the XO inhibitory potency (**8h** vs **8e**, IC_{50} = 0.0500 μM and 0.0437 μM, respectively).

Among the benzyloxy containing compounds, the insertion of the electron donating or electron withdrawing substituents, such as fluoro, chloro, bromo and methoxy substituents, at *para* position of the benzyloxy group led to a 1.3-1.8-fold increase in the inhibitory potency compared with the unsubstituted benzyloxy derivative (**8o**, **8p**, **8q**, **8r** vs **8l**, IC_{50} = 0.0507 μM, 0.0531 μM, 0.0691 μM, 0.0552 μM and 00945 μM, respectively). This finding demonstrated that modulation of the electron density of the benzyloxy aromatic ring could benefit the

inhibitory potency through introducing fluoro, chloro, bromo and methoxy substituents into the *para* position of the benzyloxy group, except compounds with a methyl or *tert*-butyl group at the *para* position of the benzyloxy group (**8m** and **8n**, IC_{50} =0.0894 μM and 0.149 μM, respectively). Then, the compounds with fluoro, chloro, bromo and methoxy groups at the *meta* position of the benzyloxy group were prepared (**8t**, **8u** and **8t**, IC_{50} = 0.0477 μM, 0.0288 μM and 0.0450 μM, respectively). Interestingly, the chloro substitution at the *meta* position, as in the case of compound **8u**, showed a remarkable inhibitory potency (IC_{50} = 0.0288 μM), 2.4-fold higher than that of compound **8p** with chloro substitution at the *para* position (IC_{50} = 0.0691 μM), which indicated that a chlorine atom substituted at the *meta* position of the benzyloxy group was beneficial for increasing the inhibitory potency. To further examine the influence of the positions and number of chlorine atoms on the benzyloxy group, the corresponding *ortho*-monochloro, *ortho* and *para*-dichloro and *ortho*-dichloro substituted derivatives were synthesized (**8w**, **8x** and **8y**, IC_{50} = 0.0917 μM, 0.0639 μM and 0.0838 μM, respectively). Among them, the *ortho* substituted derivative **8w** showed a 3.2-fold decrease in inhibitory potency in comparison to compound **8u** (**8w** < **8u**, IC_{50} = 0.0917 μM and 0.0288 μM, respectively), and the dichloro substituted derivatives also had a slight decrease in the inhibitory potency (**8x**, **8y** < **8u**, IC_{50} = 0.0639 μM, 0.0838 μM and 0.0288 μM, respectively). Presumably, the chloro monosubstitution at the *meta* position kept the chlorobenzyloxy moiety in a more favorable position so that it could form better hydrophobic interactions with nonpolar residues at the entrance of the XO active pocket.

Compound **8z** has a polar hydroxy group substituted at the 4′-position, and it showed an IC_{50} value of 629 μM, which was 4.2-21.8-fold weaker than those of other compounds (**8a**-**8y**) with hydrophobic alkoxy groups substituted at the 4′-position. In addition, the hydrophobic group at the 4′-position was indispensable for the inhibitory potency *in vitro* against XO, and this finding was consistent with the conclusion of the isocytosine derivatives [22].

2.3. Molecular modeling

To explore a probable interaction model of inhibitors and the XO active site, molecular docking of the compound **8u** in the substrate binding pocket of XO was performed using the Glide XP docking protocol (2016, Schrodinger Suite). Since molybdenum-pterion sites of both XO and bovine xanthine dehydrogenase (XDH) are structurally equivalent [58], the X-ray crystal structure of the XDH/febuxostat complex (PDB code 1N5X) used

in the docking studies was obtained from the RCSB Protein Data Bank (PDB) [16]. The protein was prepared by removing all water molecules and adding all hydrogen atoms using Protein Preparation Wizard (2016, Schrodinger Suite). The carboxyl groups of compound **8u** and febuxostat were calculated in dissociated forms using the LIGPREP module (2016, Schrodinger Suite).

The binding model of the representative compound **8u** was illustrated by Discovery Studio Visualizer 2017 and Pymol (**Fig. 4**). According to our docking studies, the binding site residues and overall binding mode of **8u** were similar to that observed with febuxostat (**Fig. 4a, Fig. 4b**), and the results showed that the tetrazole moiety of the phenyl unit was able to be accommodated by the subpocket formed by Leu648, Asn768, Lys771, Leu1014 and Pro1076, which further interacted with Asn768 and Lys771 through two hydrogen bonds, as expected (**Fig. 4c**). In the deepest part of the channel, the carbonyl group of the pyrimidine engaged in two hydrogen bonds with the side chain hydroxy group of Thr1010 and the backbone amino group of Thr1010 and two additional hydrogen bonds with the guanidine group of Arg880. Moreover, the carboxyl group of the pyrimidine formed an electrostatic interaction and a hydrogen bond with Arg880 and two additional hydrogen bonds with Mo-OH. The pyrimidine ring as a whole was sandwiched between Phe914 and Phe1009 via "face-to-face" and "face-to-edge" π-π stacking interactions, respectively. In addition, the N-3 atom of the pyrimidine acted as a H-bond acceptor and linked to the amino acid residue Glu802 via a hydrogen bond. Furthermore, several hydrophobic interactions, including a strong π-π interaction between Phe649 and the 3-chlorobenzyl group of the phenyl unit, were also observed at the mouth of the pocket with Leu648, Phe649, Leu873, Val1011 and Leu1014 (**Fig. 4c**).

As designed, the carbonyl group, which exercised a role similar to the carboxyl group of febuxostat, was able to interact simultaneously with Thr1010 and Arg880. Meanwhile, the carboxyl group was closer to the deep part of the active pocket, still retaining the key interactions with Arg880 and surprisingly increasing two extra hydrogen bonds with Mos3004.

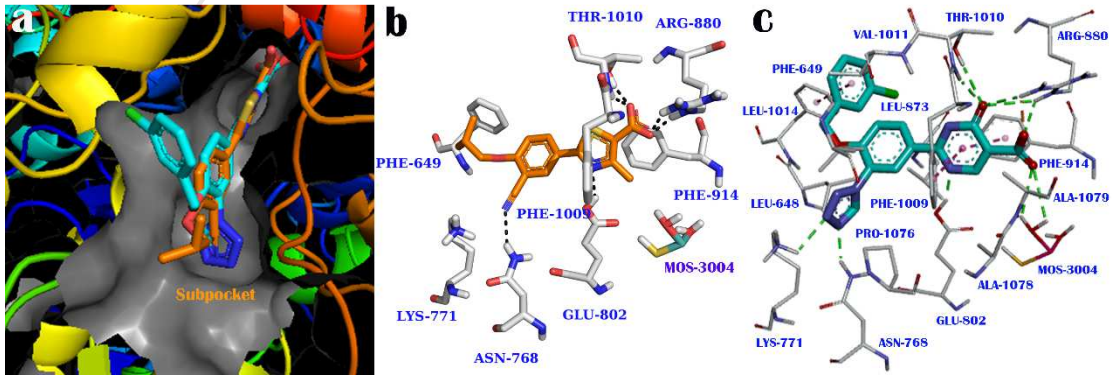

Fig. 4. Binding modes of **8u** and febuxostat within the XO binding pocket. (a) Protein (PDB code 1N5X,

rainbow) is shown as a cartoon, and small molecules are shown as a line. The subpocket of the binding pocket is shown as a surface colored in gray. **8u** (cyan) and febuxostat (orange) occupy the same binding site in XO. (b) XO residues interacting with febuxostat are depicted by gray lines. Hydrogen bonds of febuxostat are shown as black dashed lines. (c) XO residues interacting with **8u** (cyan) are depicted by gray lines. Hydrogen bonds, electrostatic interactions and π-π stacking interactions of **8u** are shown as green, orange and purple dashed lines, respectively.

2.4. Steady-state kinetic analysis

To determine the action mode of compounds **8a-8z** with XO, enzyme kinetics studies of the representative compound **8u** were performed (**Fig. 5**). As show in **Fig.5**, the analysis on the data of compound 8u indicated that V_{max} decreased with changing slope (K_m/V_{max}) in the presence of increasing concentrations of inhibitor, wherein, the K_m and V_{max} values in the presence of 0.0133 to 0.106 μM compound **8u** were 11.48, 24.63, 44.17, 74.54 μM and 0.151, 0.141, 0.124, 0.0961 μM /min, while, for the positive control, the K_m and V_{max} values were 5.33 μM and 0.155 μM /min, respectively. This behavior showed that **8u** acted as a mixed-type mode inhibitor with respect to xanthine for binding to XO, which was similar to febuxostat. Moreover, it was found that the intersecting lines on the graph converge to the second quadrant, which indicated that the value of α (a constant that defines the degree to which inhibitor binding affects the affinity of the enzyme for the substrate) was greater than 1 [6,8]. This confirmed that the inhibitor preferentially bound to the free enzyme and not the enzyme–substrate complex. In addition, dose-dependent inhibition of XO by **8u** was exhibited (**Fig. 6**).

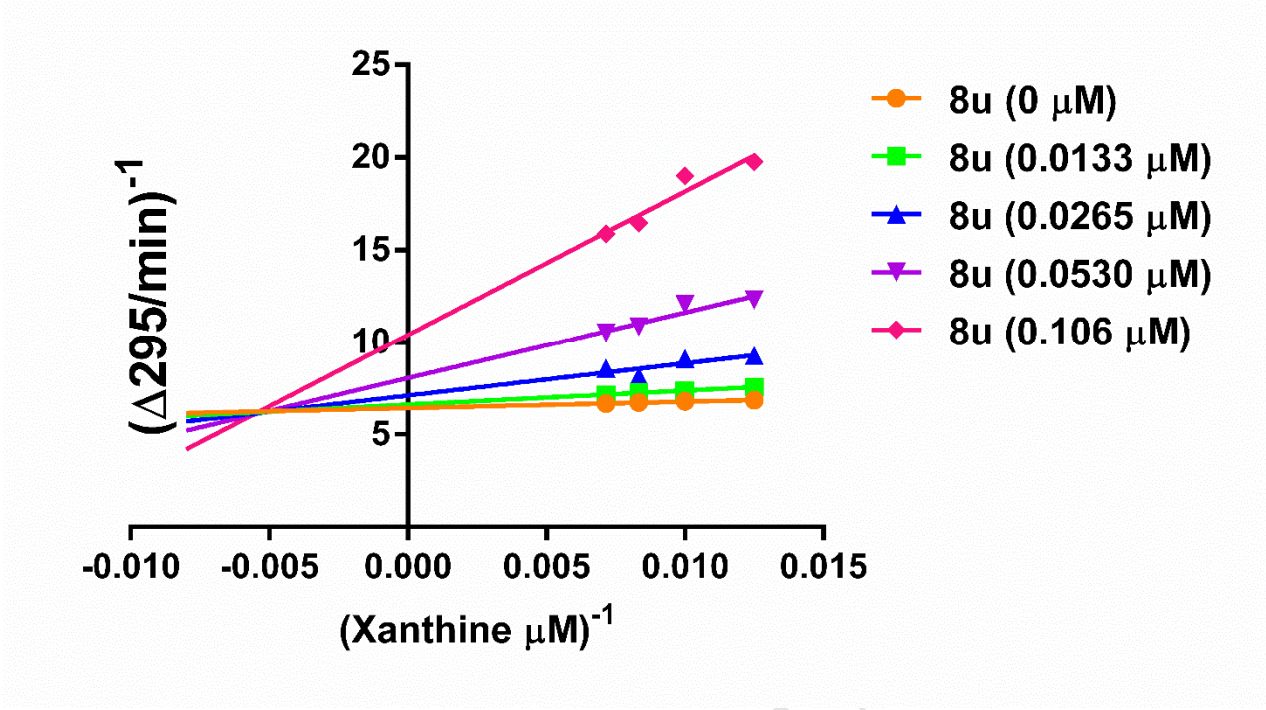

Fig. 5. Lineweaver-Burk plots of XO inhibition by compound **8u.**

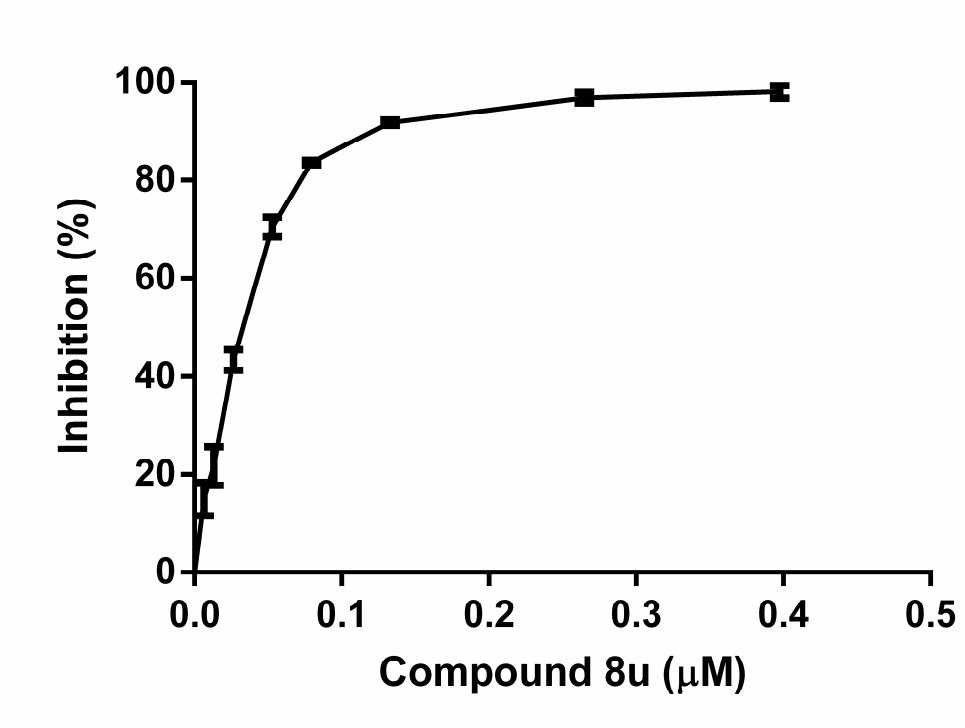

Fig. 6. The inhibition of XO by compound **8u**. Values are means ± SDs, n = 3.

2.5. Acute oral toxicity study

To explore the preliminary toxicity profile of the most potent compound **8u**, the acute oral toxicity study was performed at dose up to 2000 mg/kg, which was about 400 times over the effective dose of 5mg/kg**,** according to OECD guidelines 2001 [59]. No signs and symptoms of toxicity and mortality were observed within 24 h after the administration of test compound.

2.6. Hypouricemic effect in vivo

Since the compound **8u** showed more potent inhibitory activity than all other compounds tested *in vitro*, its *in vivo* hypouricemic effect in the acute hyperuricemia rat model was investigated and compared with those of febuxostat and allopurinol (**Fig. 7**). As expected, an intraperitoneal injection of 300 mg/kg potassium oxonate markedly increased serum uric acid levels 3 h after drug administration in the model group compared with the blank group ($P < 0.001$ for **Blank** vs **Model**), confirming that the model was successfully established. In addition, administration of a single oral dose of 5 mg/kg **8u** was able to significantly reduce the serum levels of uric acid at 3 h ($P < 0.05$ for **8u** vs **Model**), although the hypouricemic action was slightly lower than that of febuxostat and allopurinol at an oral dose of 5 mg/kg and 10 mg/kg, respectively. Furthermore, the compound **8u** was able to reduce the serum uric acid levels comparable to the blank group from 3 h to 8 h (①$P > 0.05$ for **8u** vs **Blank**). The results of *in vivo* hypouricemic activity evaluation suggested that compound **8u** was a potential and efficacious agent in the treatment of hyperuricemia.

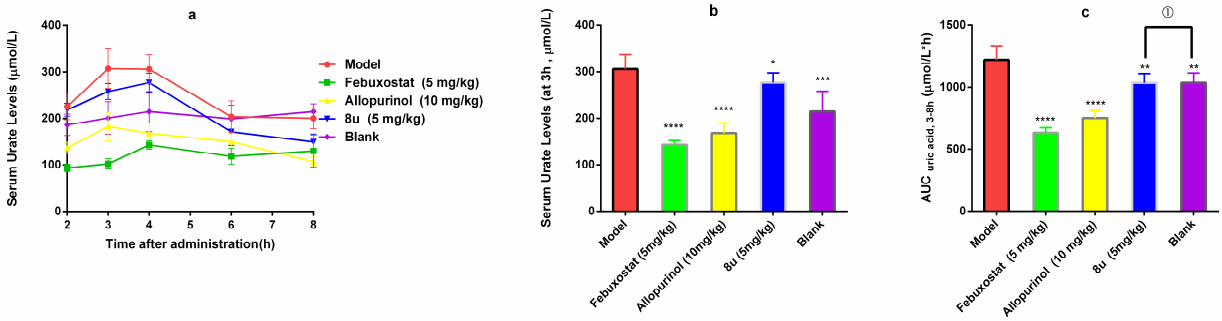

Fig. 7. Effect of compound **8u**, febuxostat and allopurinol on the serum uric acid levels in the potassium oxonate-induced hyperuricemic rat model. (a) Time course changes in the serum uric acid levels after oral administration of Febuxostat, Allopurinol and **8u** in a potassium oxonate induced hyperuricemic rat. (b) The serum uric acid levels 3 h after oral administration of Febuxostat, Allopurinol and **8u** in a potassium oxonate induced hyperuricemic rat. (c) The $AUC_{(uric\ acid,\ 3\text{-}8\ h)}$ after oral administration of **8u**, febuxostat and allopurinol in

a potassium oxonate induced hyperuricemic rat. Data are expressed as the mean ± S.D. *P < 0.05, *P < 0.001 and ****P < 0.0001 vs hyperuricemic rat (**model**), ①P>0.05 vs **Blank**.

3. Conclusion

We designed, synthesized and identified a series of 2-[4-alkoxy-3-(1*H*-tetrazol-1-yl) phenyl]-6-oxo-1,6-dihydropyrimidine-5-carboxylic acid derivatives as novel XO inhibitors with a tetrazole group targeting the subpocket formed by residues Leu648, Asn768, Lys771, Leu1014 and Pro1076 at the XO active site. Specifically, compound **8u**, which was comparable to febuxostat, emerged as the most potent XO inhibitor. The Lineweaver-Burk plot showed that compound **8u** acted as a mixed-type XO inhibitor. The structure-activity relationship analysis demonstrated that the hydrophobic group at the 4′-position was indispensable for the inhibitory potency *in vitro* against XO. Furthermore, molecular docking studies provided the molecular basis for rationalizing the activity of the designed compounds and suggested that the subpocket centered around Asn768 was able to accommodate the tetrazole group, which further provided a potential strategy for the design of nonpurine XO inhibitors. The results of *in vivo* hypouricemic activity evaluation suggested that compound **8u** could effectively reduce serum uric acid levels at an oral dose of 5 mg/kg. In addition, acute oral toxicity study in mice indicated that compound **8u** was nontoxic and tolerated at dose up to 2000 mg/kg. Thus, compound **8u** could be a potential and efficacious agent in treatment of hyperuricemia with low toxicity.

4. Experimental protocols

4.1 Chemistry

Unless otherwise indicated, reagents and solvents were purchased from commercial sources and used without further purification. All reactions were monitored by TLC using silica gel aluminum cards (0.2 mm thickness) with 254 nm and 365 nm fluorescent indicator. Melting points were recorded on a YRT-3 melting apparatus and were uncorrected. ^{1}H NMR spectra were recorded on a Bruker 400 MHz spectrometer or a Bruker

600 MHz spectrometer, and ^{13}C NMR spectra were recorded on a Bruker 400 MHz spectrometer or a Bruker 600 MHz spectrometer. Chemical shifts were expressed in parts per million using tetramethylsilane as an internal reference and DMSO-d_6 as the solvent. IR spectra were determined as KBr pellets on a Bruker IFS-55 spectrometer and expressed in reciprocal centimeters. ESI-MS data were gathered using an Agilent 1100 instrument. ESI-HRMS data were recorded in the Agilent 6540 Series Q-TOF-MS system.

*4.1.1. Synthesis of 4-hydroxy-3-nitrobenzonitrile (**2**)*

A solution of nitric acid (24.4 g, 0.252 mol) in acetic acid (80 mL) was added dropwise at 75 ℃ to a stirred solution of 4-hydroxybenzonitrile (30.0 g, 0.252 mol) in acetic acid (200 mL). Upon completion of the addition, the mixture was heated under reflux for anther 1 h, then it was poured into ice water, and the precipitate was filtered, washed with water to yield the compound **2** (39.0 g, 94.2%) as a yellow solid, mp 144.2°C-145.6°C. MS (ESI) m/z: 163.0 $[M - H]^-$; ^{1}H NMR (600 MHz, DMSO-d_6) δ 12.34 (s, 1H), 8.42 (d, J = 2.1 Hz, 1H), 7.94 (dd, J = 8.7, 2.1 Hz, 1H), 7.24 (d, J = 8.7 Hz, 1H).

*4.1.2. Synthesis of 3-amino-4-hydroxybenzonitrile (**3**)*

A mixture of the compound **2** (39.0 g, 0.238 mol) and 10% Pd/C (3.9 g) in methanol was stirred at room temperature for 12 h under hydrogen atmosphere. After the completion of the reaction, the Pd/C was filtered out and the filtrate was evaporated to give a brown solid (29.5 g, 92.3%), which was used directly in the next step. Mp 135.6 ℃-136.6 ℃. MS (ESI) m/z: 480.8 $[2M + Na]^+$; ^{1}H NMR (600 MHz, DMSO-d_6) δ 9.79 (s, 1H), 8.26 (d, J = 2.1 Hz, 1H), 8.07 (dd, J = 8.8, 2.1 Hz, 1H), 7.58 (d, J = 8.9 Hz, 1H), 4.92 (hept, J = 6.0 Hz, 1H), 1.27 (d, J = 6.0 Hz, 6H).

*4.1.3. Synthesis of 4-hydroxy-3-(1H-tetrazol-1-yl) benzonitrile (**4**)*

A mixture of 4-hydroxy-3-nitro benzonitrile (29.5 g, 0.220 mol), triethyl orthoformate (39.1 g, 0.264 mol) and sodium azide (14.4 g, 0.222 mol) was added to acetic acid (88.5 mL). The mixture was stirred at 60 ℃ for 12 h under nitrogen atmosphere. After completion of the reaction, the precipitate was filtered and recrystallized from ethanol to give the compound **4** (21.53 g, 52.3%) as a gray white solid, mp 194.8°C-195.0°C. MS (ESI) m/z: 185.9 $[M - H]^-$; ^{1}H NMR (600 MHz, DMSO-d_6) δ 12.15 (s, 1H), 9.83 (s, 1H), 8.20 (d, J = 2.1 Hz, 1H), 7.89 (dd, J = 8.6, 2.1 Hz, 1H), 7.26 (d, J = 8.6 Hz, 1H).

*4.1.4. Synthesis of 4-methoxy-3-(1H-tetrazol-1-yl) benzonitrile (**5a**)*

A mixture of the compound **4** (6 g, 32.06 mmol), methyl iodide (5.46 g, 38.47 mmol), anhydrous potassium carbonate (8.85 g, 42.7 mmol) and DMF (32 mL) was reacted at ambient temperature for 6 h under nitrogen atmosphere. After the reaction was completed, the mixture was poured into water (200 mL). The precipitate was filtered, washed with water, and recrystallized (petroleum ether : ethyl acetate = 1:2) to yield the compound **5a** (3.65 g, 39.1%) as a white solid, mp 172.3 °C-174.1 °C . MS (ESI) m/z: 202.4 $[M + H]^+$; 224.4 $[M + Na]^+$; ^{1}H NMR (600 MHz, DMSO-d_6) δ 9.85 (s, 1H), 8.28 (d, *J* = 2.1 Hz, 1H), 8.12 (dd, *J* = 8.8, 2.1 Hz, 1H), 7.56 (d, *J* = 8.8 Hz, 1H), 3.96 (s, 3H).

*4.1.5. General procedure for synthesis of 4-alkoxy-3-(1H-tetrazol-1-yl) benzonitriles (**5b-5y**)*

A mixture of compound **4** (6 g, 32.06 mmol), alkyl halides or benzyl halides (38.47 mmol), anhydrous potassium carbonate (8.85 g, 42.7 mmol), potassium iodide (710.48 mg, 4.28 mmol) and DMF (32 mL) was reacted at 50°C for 8 h under nitrogen atmosphere. After the reaction was completed, the mixture was poured into water (200 mL). The precipitate was filtered, washed with water, and recrystallized (petroleum ether: ethyl acetate = 1:2) to yield 4-alkoxy-3-(1*H*-tetrazol-1-yl) benzonitriles (**5b**-**5y**).

*4.1.5.1. Synthesis of 4-isopropoxy-3-(1H-tetrazol-1-yl) benzonitrile (**5b**)*

A white solid, yield: 66.5%. Mp 135.6 °C-136.6 °C. MS (ESI) m/z: 480.8 $[2M + Na]^+$; ^{1}H NMR (600 MHz, DMSO-d_6) δ 9.79 (s, 1H), 8.26 (d, *J* = 2.1 Hz, 1H), 8.07 (dd, *J* = 8.8, 2.1 Hz, 1H), 7.58 (d, *J* = 8.9 Hz, 1H), 4.92 (hept, *J* = 6.0 Hz, 1H), 1.27 (d, *J* = 6.0 Hz, 6H).

*4.1.5.2. Synthesis of 4-isobutoxy-3-(1H-tetrazol-1-yl) benzonitrile (**5c**)*

A white solid, yield: 69.3%. Mp 139.2 °C-140.6 °C. MS (ESI) m/z: 244.4 $[M + H]^+$; 266.3 $[M + Na]^+$; 508.9 $[2M + Na]^+$; ^{1}H NMR (600 MHz, DMSO-d_6) δ 9.79 (s, 1H), 8.28 (d, *J* = 2.1 Hz, 1H), 8.10 (dd, *J* = 8.8, 2.1 Hz, 1H), 7.54 (d, *J* = 8.8 Hz, 1H), 3.98 (d, *J* = 6.3 Hz, 2H), 1.95 (hept, *J* = 6.6 Hz, 1H), 0.84 (d, *J* = 6.7 Hz, 6H).

*4.1.5.3. Synthesis of 4-(isopentyloxy)-3-(1H-tetrazol-1-yl) benzonitrile (**5d**)*

A white solid, yield: 81.9%. Mp 108.7 °C-190 °C. MS (ESI) m/z: 258.3 $[M + H]^+$; 280.2 $[M + Na]^+$; 536.8 $[2M + Na]^+$; ^{1}H NMR (600 MHz, DMSO-d_6) δ 9.79 (s, 1H), 8.27 (d, *J* = 2.1 Hz, 1H), 8.10 (dd, *J* = 8.8, 2.1 Hz, 1H), 7.57 (d, *J* = 8.8 Hz, 1H), 4.22 (t, *J* = 6.3 Hz, 2H), 1.57 (dq, *J* = 12.2, 6.0 Hz, 3H), 0.83 (d, *J* = 6.3 Hz, 6H).

*4.1.5.4. Synthesis of 4-(allyloxy)-3-(1H-tetrazol-1-yl) benzonitrile (**5e**)*

A white solid, yield: 94.5%. Mp 112.4°C-113.5°C. MS (ESI) m/z: 228.3 $[M + H]^+$; 250.2 $[M + Na]^+$; 476.9 $[2M + Na]^+$; ^{1}H NMR (600 MHz, DMSO-*d*6) δ 9.84 (s, 1H), 8.29 (d, *J* = 2.0 Hz, 1H), 8.11 (dd, *J* = 8.8, 2.0 Hz, 1H), 7.54 (d, *J* = 8.8 Hz, 1H), 5.98 (ddt, *J* = 15.8, 10.4, 5.1 Hz, 1H), 5.31 – 5.23 (m, 2H), 4.81 (d, *J* = 5.1 Hz, 2H).

*4.1.5.5. Synthesis of 4-[(2-methylallyl) oxy]-3-(1H-tetrazol-1-yl) benzonitrile (**5f**)*

A white solid, yield: 85.4%. Mp 115.9°C -117.5°C. MS (ESI) m/z : 242.3 $[M + H]^+$; 264.2 $[M + Na]^+$; 504.8 $[2M + Na]^+$; ^{1}H NMR (600 MHz, DMSO-d_6) δ 9.81 (s, 1H), 8.30 (d, *J* = 2.0 Hz, 1H), 8.11 (dd, *J* = 8.8, 2.0 Hz, 1H), 7.53 (d, *J* = 8.8 Hz, 1H), 4.92 (d, *J* = 19.0 Hz, 2H), 4.71 (s, 2H), 1.65 (s, 3H).

*4.1.5.6. Synthesis of 4-[(3-methylbut-2-en-1-yl) oxy]-3-(1H-tetrazol-1-yl) benzonitrile (**5g**)*

A white solid, yield: 70.2%. Mp 126.3°C-127.2°C. MS (ESI) m/z: 256.2 $[M + H]^+$; 278.2 $[M + Na]^+$; 532.8 $[2M + Na]^+$; ^{1}H NMR (600 MHz, DMSO-d_6) δ 9.79 (s, 1H), 8.26 (d, *J* = 2.0 Hz, 1H), 8.09 (dd, *J* = 8.8, 2.0 Hz, 1H), 7.55 (d, *J* = 8.8 Hz, 1H), 5.37 (t, *J* = 6.6 Hz, 1H), 4.78 (d, *J* = 6.7 Hz, 2H), 1.69 (d, *J* = 23.2 Hz, 6H).

*4.1.5.7. Synthesis of 4-(prop-2-yn-1-yloxy)-3-(1H-tetrazol-1-yl) benzonitrile (**5h**)*

A brown solid, yield: 82.4%. Mp 138.4°C-138.9°C. ^{1}H NMR (600 MHz, DMSO-d6) δ 9.83 (s, 1H), 8.37 – 8.27 (m, 1H), 8.21 – 8.12 (m, 1H), 7.61 (d, *J* = 8.8 Hz, 1H), 5.15 – 5.03 (m, 2H), 3.74 (d, *J* = 2.6 Hz, 1H).

*4.1.5.8. Synthesis of 4-(cyclopropylmethoxy)-3-(1H-tetrazol-1-yl) benzonitrile (**5i**)*

A brown solid, yield: 91.3%. Mp 139.1°C-140.2°C. ^{1}H NMR (600 MHz, DMSO-d_6) δ 9.81 (s, 1H), 8.28 (d, *J* = 2.1 Hz, 1H), 8.07 (dd, *J* = 8.7, 2.1 Hz, 1H), 7.52 (d, *J* = 8.8 Hz, 1H), 4.09 (d, *J* = 7.1 Hz, 2H), 1.20 (dddd, *J* = 15.1, 10.3, 5.3, 2.4 Hz, 1H), 0.56 – 0.49 (m, 2H), 0.34 – 0.27 (m, 2H).

*4.1.5.9. Synthesis of 4-(cyclopentyloxy)-3-(1H-tetrazol-1-yl) benzonitrile (**5J**)*

A white solid, yield: 64.3%. Mp 148°C-149.1°C. MS (ESI) m/z: 256.3 $[M + H]^+$; 278.2 $[M + Na]^+$; ^{1}H NMR (600 MHz, DMSO-d_6) δ 9.75 (s, 1H), 8.26 (d, *J* = 2.1 Hz, 1H), 8.07 (dd, *J* = 8.8, 2.1 Hz, 1H), 7.54 (d, *J* = 8.8 Hz, 1H), 5.11 (tt, *J* = 5.6, 2.5 Hz, 1H), 1.95 – 1.82 (m, 2H), 1.71 – 1.62 (m, 2H), 1.59 – 1.47 (m, 4H).

*4.1.5.10. Synthesis of 4-(cyclohexylmethoxy)-3-(1H-tetrazol-1-yl) benzonitrile (**5k**)*

A white solid, yield: 63.2%. Mp 120.6°C-122.2°C. ^{1}H NMR (600 MHz, DMSO-d_6) δ 9.78 (s, 1H), 8.27 (d, *J* = 2.1 Hz, 1H), 8.09 (dd, *J* = 8.8, 2.1 Hz, 1H), 7.54 (d, *J* = 8.8 Hz, 1H), 4.01 (d, *J* = 6.2 Hz, 2H), 1.71 – 1.56 (m, 6H), 1.17 (qt, *J* = 12.3, 3.2 Hz, 2H), 1.07 (qt, *J* = 12.6, 3.2 Hz, 1H), 0.91 (qd, *J* = 12.4, 3.4 Hz, 2H).

*4.1.5.11. Synthesis of 4-(benzyloxy)-3-(1H-tetrazol-1-yl) benzonitrile (**5l**)*

A white solid, yield: 66.6%. Mp 148.3°C-149.0°C. MS (ESI) m/z: 576.8 $[2M + Na]^+$; ^{1}H NMR (600 MHz, DMSO-d_6) δ 9.83 (s, 1H), 8.31 (d, *J* = 2.1 Hz, 1H), 8.12 (dd, *J* = 8.8, 2.1 Hz, 1H), 7.63 (d, *J* = 8.8 Hz, 1H), 7.41 – 7.31 (m, 6H), 5.36 (s, 2H).

*4.1.5.12. Synthesis of 4-[(4-methylbenzyl) oxy]-3-(1H-tetrazol-1-yl) benzonitrile (**5m**)*

An off-white solid, yield: 96.5%. Mp 161.2°C-162.5°C. MS (ESI) m/z : 604.6 $[2M + Na]^+$; ^{1}H NMR (600 MHz, DMSO-d_6) δ 9.80 (s, 1H), 8.29 (d, *J* = 2.1 Hz, 1H), 8.11 (dd, *J* = 8.8, 2.1 Hz, 1H), 7.62 (d, *J* = 8.8 Hz, 1H), 7.26 (d, *J* = 8.0 Hz, 2H), 7.18 (d, *J* = 7.8 Hz, 2H), 5.29 (s, 2H), 2.28 (s, 3H).

*4.1.5.13. Synthesis of 4-{[4-(tert-butyl) benzyl] oxy}-3-(1H-tetrazol-1-yl) benzonitrile (**5n**)*

An off-white solid, yield: 80.2%. Mp 125.6 °C-128.4 °C. MS (ESI) m/z: 356.4 $[M + Na]^+$; ^{1}H NMR (600 MHz, DMSO-d_6) δ 9.84 (s, 1H), 8.30 (d, *J* = 2.1 Hz, 1H), 8.12 (dd, *J* = 8.8, 2.1 Hz, 1H), 7.65 (d, *J* = 8.8 Hz, 1H), 7.42 – 7.37 (m, 2H), 7.33 – 7.26 (m, 2H), 5.32 (s, 2H), 1.26 (s, 9H).

*4.1.5.14. Synthesis of 4-[(4-methoxybenzyl) oxy]-3-(1H-tetrazol-1-yl) benzonitrile (**5o**)*

A white solid, yield: 68.4%. Mp 148.9°C-150.2°C. MS (ESI) m/z: 330.2 $[M + Na]^+$; ^{1}H NMR (600 MHz, DMSO-d_6) δ 9.79 (s, 1H), 8.29 (d, *J* = 2.0 Hz, 1H), 8.12 (dd, *J* = 8.8, 2.1 Hz, 1H), 7.64 (d, *J* = 8.8 Hz, 1H), 7.33 (d, *J* = 8.6 Hz, 2H), 6.93 (d, *J* = 8.6 Hz, 2H), 5.26 (s, 2H), 3.74 (s, 3H).

*4.1.5.15. Synthesis of 4-[(4-fluorobenzyl) oxy]-3-(1H-tetrazol-1-yl) benzonitrile (**5p**)*

A white solid, yield: 52.7%. Mp 160.7°C-161.6°C. MS (ESI) m/z: 296.4 $[M + H]^+$; 318.2 $[M + Na]^+$; ^{1}H NMR (600 MHz, DMSO-d_6) δ 9.83 (s, 1H), 8.30 (d, *J* = 2.0 Hz, 1H), 8.12 (dd, *J* = 8.8, 2.0 Hz, 1H), 7.63 (d, *J* = 8.8 Hz, 1H), 7.45 (dd, *J* = 8.4, 5.6 Hz, 2H), 7.21 (t, *J* = 8.8 Hz, 2H), 5.34 (s, 2H).

*4.1.5.16. Synthesis of 4-[(4-chlorobenzyl) oxy]-3-(1H-tetrazol-1-yl) benzonitrile (**5q**)*

A white solid, yield: 61.1%. Mp 195.9°C-197°C. ^{1}H NMR (600 MHz, DMSO-d_6) δ 9.84 (s, 1H), 8.31 (d, *J* = 2.0 Hz, 1H), 8.12 (dd, *J* = 8.8, 2.0 Hz, 1H), 7.61 (d, *J* = 8.8 Hz, 1H), 7.45 (d, *J* = 8.4 Hz, 2H), 7.41 (d, *J* = 8.4 Hz, 2H), 5.35 (s, 2H).

*4.1.5.17. Synthesis of 4-[(4-bromobenzyl) oxy]-3-(1H-tetrazol-1-yl) benzonitrile (**5r**)*

A white solid, yield: 59.4%. Mp 181.3°C-183.6°C. MS (ESI) m/z: 373.1 $[M + H]^+$; 395.2 $[M + Na]^+$; ^{1}H NMR (600 MHz, DMSO-d_6) δ 9.84 (s, 1H), 8.31 (d, *J* = 1.8 Hz, 1H), 8.12 (dd, *J* = 8.8, 1.8 Hz, 1H), 7.61 (d, *J* = 8.8 Hz, 1H), 7.58 (d, *J* = 8.3 Hz, 2H), 7.34 (d, *J* = 8.2 Hz, 2H), 5.34 (s, 2H).

*4.1.5.18. Synthesis of 4-[(3-methoxybenzyl) oxy]-3-(1H-tetrazol-1-yl) benzonitrile (**5s**)*

A white solid, yield: 85.6%. Mp 134.4°C-135.6°C .MS (ESI) m/z: 308.3 $[M + H]^+$; 330.2 $[M + Na]^+$; ^{1}H NMR (400 MHz, DMSO-d_6) δ 9.85 (s, 1H), 8.31 (d, *J* = 2.1 Hz, 1H), 8.12 (dd, *J* = 8.8, 2.1 Hz, 1H), 7.61 (d, *J* = 8.8 Hz, 1H), 7.28 (t, 1H), 6.97 – 6.85 (m, 3H), 5.33 (s, 2H), 3.73 (s, 3H).

*4.1.5.19. Synthesis of 4-[(3-fluorobenzyl) oxy]-3-(1H-tetrazol-1-yl) benzonitrile (**5t**)*

An off-white solid, yield: 87.0%. Mp 142.6°C -144.7°C .MS (ESI) m/z: 296.3 $[M + H]^+$; 318.2 $[M + Na]^+$; ^{1}H NMR (400 MHz, DMSO-d_6) δ 9.87 (s, 1H), 8.31 (d, *J* = 2.1 Hz, 1H), 8.13 (dd, *J* = 8.8, 2.2 Hz, 1H), 7.61 (d, *J* = 8.8 Hz, 1H), 7.49 – 7.38 (m, 1H), 7.24 – 7.19 (m, 2H), 7.19 – 7.13 (m, 1H), 5.38 (s, 2H).

*4.1.5.20. Synthesis of 4-[(3-chlorobenzyl) oxy]-3-(1H-tetrazol-1-yl) benzonitrile (**5u**)*

An off-white solid, yield: 54.3%. Mp 157.2°C-158.5°C. ^{1}H NMR (600 MHz, DMSO-d_6) δ 9.88 (s, 1H), 8.32 (d, *J* = 2.1 Hz, 1H), 8.14 (dd, *J* = 8.8, 2.1 Hz, 1H), 7.61 (d, *J* = 8.8 Hz, 1H), 7.46 (d, *J* = 2.0 Hz, 1H), 7.44 – 7.38 (m, 2H), 7.34 (dd, *J* = 5.0, 3.4 Hz, 1H), 5.37 (s, 2H).

*4.1.5.21. Synthesis of 4-[(3-bromobenzyl) oxy]-3-(1H-tetrazol-1-yl) benzonitrile (**5v**)*

An off-white solid, yield: 66.5%. Mp 161.9 °C -162.2 °C. MS (ESI) m/z: 378.2 $[M + Na]^+$; ^{1}H NMR (600 MHz, DMSO-d_6) δ 9.87 (s, 1H), 8.32 (d, *J* = 2.1 Hz, 1H), 8.14 (dd, *J* = 8.8, 2.1 Hz, 1H), 7.64 – 7.57 (m, 2H), 7.54 (dt, *J* = 7.5, 1.8 Hz, 1H), 7.40 – 7.31 (m, 2H), 5.36 (s, 2H).

*4.1.5.22. Synthesis of 4-[(2-chlorobenzyl) oxy]-3-(1H-tetrazol-1-yl) benzonitrile (**5w**)*

A white solid, yield: 63.5%. Mp 149.5°C-151.7°C. MS (ESI) m/z: 644.8 $[2M + Na]^+$; ^{1}H NMR (400 MHz, DMSO-d_6) δ 9.75 (s, 1H), 8.32 (d, *J* = 2.1 Hz, 1H), 8.15 (dd, *J* = 8.7, 2.1 Hz, 1H), 7.70 (d, *J* = 8.8 Hz, 1H), 7.50 (dd, *J* = 7.7, 1.6 Hz, 1H), 7.45 (dd, *J* = 7.1, 2.2 Hz, 1H), 7.43 – 7.32 (m, 2H), 5.41 (s, 2H).

*4.1.5.23. Synthesis of 4-[(2, 6-dichlorobenzyl) oxy]-3-(1H-tetrazol-1-yl) benzonitrile (**5x**)*

A white solid, yield: 83.8%. Mp 178.0°C-178.9°C. MS (ESI) m/z: 368.4 $[M + Na]^+$; ^{1}H NMR (400 MHz, DMSO-d_6) δ 9.57 (s, 1H), 8.32 (d, *J* = 2.1 Hz, 1H), 8.20 (dd, *J* = 8.7, 2.1 Hz, 1H), 7.86 (d, *J* = 8.8 Hz, 1H), 7.56 – 7.50 (m, 2H), 7.48 – 7.42 (m, 1H), 5.48 (s, 2H).

*4.1.5.24. Synthesis of 4-[(2, 4-dichlorobenzyl) oxy]-3-(1H-tetrazol-1-yl) benzonitrile (**5y**)*

A white solid, yield: 92.2%. Mp 176.7°C-177.3°C. ^{1}H NMR (400 MHz, DMSO-d_6) δ 9.75 (s, 1H), 8.32 (d, *J* = 2.1 Hz, 1H), 8.14 (dd, *J* = 8.8, 2.1 Hz, 1H), 7.76 – 7.63 (m, 2H), 7.54 – 7.41 (m, 2H), 5.40 (s, 2H).

*4.1.6. General procedure for synthesis of 4-alkoxy-3-(1H-tetrazol-1-yl) benzimidamide hydrochloride (**6a-6y**)*

A 500 mL flask was charged with 250 mL of anhydrous methanol, 17.40 mmol of the compounds **5a**-**5y**, and 5.22 mmol of sodium methoxide. The complex was protected from moisture and stirred for 36 h. Then, 34.8 mmol NH_4Cl was added and stirring was continued at 50°C for 6 h. Unreacted NH_4Cl was filtered, and the reaction mixture was concentrated under reduced pressure. The crude residue was refluxed with ethyl acetate and the precipitate was collected by filtration to give the compounds **6a-6y**, which were used for the next reaction without further purification.

*4.1.6.1. Synthesis of 4-methoxy-3-(1H-tetrazol-1-yl) benzimidamide hydrochloride (**6a**)*

A white solid, yield: 31.8%. MS (ESI) m/z: 218.2 $[M + H]^+$; ^{1}H NMR (600 MHz, DMSO-d_6) δ 9.96 (s, 1H), 9.22 (s, 3H), 8.35 (d, *J* = 2.4 Hz, 1H), 8.24 (dd, *J* = 8.9, 2.5 Hz, 1H), 7.64 (d, *J* = 9.0 Hz, 1H), 4.01 (s, 3H).

*4.1.6.2. Synthesis of 4-isopropoxy-3-(1H-tetrazol-1-yl) benzimidamide hydrochloride (**6b**)*

A white solid, yield: 24.0%. MS (ESI) m/z: 247.2 $[2M + H]^+$; 269.1 $[2M + Na]^+$ ^{1}H NMR (600 MHz, DMSO-d_6) δ 9.85 (s, 1H), 9.26 (s, 4H), 8.25 (d, *J* = 2.4 Hz, 1H), 8.08 (dd, *J* = 8.9, 2.5 Hz, 1H), 7.65 (d, *J* = 9.0

Hz, 1H), 4.96 (hept, *J* = 6.1 Hz, 1H), 1.30 (d, *J* = 6.0 Hz, 6H).

*4.1.6.3. Synthesis of 4-isobutoxy-3-(1H-tetrazol-1-yl) benzimidamide hydrochloride (**6c**)*

A white solid, yield: 61.6%. MS (ESI) m/z: 261.3 $[M + H]^+$; ^{1}H NMR (600 MHz, DMSO-d_6) δ 9.87 (s, 1H), 8.89 (s, 3H), 8.30 (d, *J* = 2.4 Hz, 1H), 8.18 (dd, *J* = 8.8, 2.5 Hz, 1H), 7.60 (d, *J* = 8.9 Hz, 1H), 4.01 (d, *J* = 6.4 Hz, 2H), 1.97 (dp, *J* = 13.2, 6.6 Hz, 1H), 0.86 (d, *J* = 6.7 Hz, 6H).

*4.1.6.4. Synthesis of 4-(isopentyloxy)-3-(1H-tetrazol-1-yl) benzimidamide hydrochloride (**6d**)*

A white solid, yield: 34.5%. MS (ESI) m/z: 275.2 $[M + H]^+$; ^{1}H NMR (600 MHz, DMSO-d_6) δ 9.86 (s, 1H), 9.14 (s, 4H), 8.28 (d, *J* = 2.4 Hz, 1H), 8.16 (dd, *J* = 8.9, 2.4 Hz, 1H), 7.64 (d, *J* = 9.0 Hz, 1H), 4.25 (t, *J* = 6.3 Hz, 2H), 1.59 (dq, *J* = 12.1, 6.1, 5.6 Hz, 3H), 0.85 (d, *J* = 6.3 Hz, 6H).

*4.1.6.5. Synthesis of 4-(allyloxy)-3-(1H-tetrazol-1-yl) benzimidamide hydrochloride (**6e**)*

A white solid, yield: 36.3%. MS (ESI) m/z: 245.1 $[M + H]^+$; 488.9 $[2M + H]^+$; 243.3 $[M - H]^-$; ^{1}H NMR (600 MHz, DMSO-d_6) δ 9.94 (s, 1H), 8.63 (s, 6H), 8.33 (s, 1H), 8.20 (d, *J* = 8.9 Hz, 1H), 7.60 (d, *J* = 8.8 Hz, 1H), 6.00 (ddt, *J* = 15.6, 9.9, 4.6 Hz, 1H), 5.28 (dd, *J* = 28.0, 13.9 Hz, 2H), 4.84 (d, *J* = 3.9 Hz, 2H).

*4.1.6.6. Synthesis of 4-[(2-methylallyl) oxy]-3-(1H-tetrazol-1-yl) benzimidamide hydrochloride (**6f**)*

A white solid, yield: 33.6%. MS (ESI) m/z: 259.1 $[M + H]^+$; 517.0 $[2M + H]^+$; 257.3 $[M - H]^-$; ^{1}H NMR (600 MHz, DMSO-d_6) δ 9.91 (s, 1H), 8.32 (d, *J* = 2.3 Hz, 1H), 8.20 (dd, *J* = 8.9, 2.4 Hz, 1H), 8.13 – 7.96 (m, 10H), 7.59 (d, *J* = 8.9 Hz, 1H), 4.93 (d, *J* = 4.0 Hz, 2H), 4.74 (s, 2H), 1.66 (s, 3H).

*4.1.6.7. Synthesis of 4-[(3-methylbut-2-en-1-yl) oxy]-3-(1H-tetrazol-1-yl) benzimidamide hydrochloride (**6g**)*

A white solid, yield: 47.3%. MS (ESI) m/z: 273.2 $[M + H]^+$; 544.9 $[2M + H]^+$; ^{1}H NMR (600 MHz, DMSO-d_6) δ 9.87 (s, 1H), 9.22 (s, 0H), 8.30 (d, 2H), 8.18 (dd, 2H), 7.61 (d, *J* = 8.9 Hz, 1H), 5.39 (s, 2H), 4.81 (d, *J* = 6.5 Hz, 3H), 1.70 (d, *J* = 17.8 Hz, 7H).

*4.1.6.8. Synthesis of 4-(prop-2-yn-1-yloxy)-3-(1H-tetrazol-1-yl) benzimidamide hydrochloride (**6h**)*

A white solid, yield: 36.7%. MS (ESI) m/z: 243.4 $[M + H]^+$; 265.3 $[M + Na]^+$; ^{1}H NMR (600 MHz, DMSO-d_6) δ 9.92 (s, 1H), 9.01 (s, 5H), 8.34 (s, 1H), 8.23 (d, *J* = 8.8 Hz, 1H), 7.66 (d, *J* = 8.9 Hz, 1H), 5.11 (s,

2H), 3.77 (s, 1H).

*4.1.6.9. Synthesis of 4-(cyclopropylmethoxy)-3-(1H-tetrazol-1-yl) benzimidamide hydrochloride (**6i**)*

A white solid, yield: 53.7%. MS (ESI) m/z: 259.3 $[M + H]^+$; ^{1}H NMR (600 MHz, DMSO-d_6) δ 9.90 (s, 1H), 8.32 (d, *J* = 2.4 Hz, 1H), 8.18 (dd, *J* = 8.9, 2.5 Hz, 1H), 7.72 (s, 29H), 7.58 (d, *J* = 8.9 Hz, 1H), 4.11 (d, *J* = 7.1 Hz, 2H), 1.27 – 1.16 (m, 1H), 0.57 – 0.48 (m, 2H), 0.35 – 0.28 (m, 2H).

*4.1.6.10. Synthesis of 4-(cyclopentyloxy)-3-(1H-tetrazol-1-yl) benzimidamide hydrochloride (**6J**)*

A white solid, yield: 26.9%. MS (ESI) m/z: 273.2 $[M + H]^+$; 295.2 $[M + Na]^+$; ^{1}H NMR (600 MHz, DMSO-d_6) δ 9.83 (s, 1H), 8.40 (s, 1H), 8.29 (d, *J* = 2.4 Hz, 1H), 8.16 (dd, *J* = 8.9, 2.4 Hz, 4H), 7.60 (d, *J* = 8.9 Hz, 1H), 5.17 – 5.13 (m, 1H), 1.97 – 1.88 (m, 2H), 1.74 – 1.65 (m, 2H), 1.60 – 1.51 (m, 4H).

*4.1.6.11. Synthesis of 4-(cyclohexylmethoxy)-3-(1H-tetrazol-1-yl) benzimidamide hydrochloride (**6k**)*

A white solid, yield: 42.5%. MS (ESI) m/z: 301.3 $[M + H]^+$; ^{1}H NMR (600 MHz, DMSO-d_6) δ 9.85 (s, 1H), 8.26 (d, *J* = 2.5 Hz, 1H), 8.14 (dd, *J* = 9.0, 2.5 Hz, 2H), 7.96 (s, 10H), 7.61 (d, *J* = 8.9 Hz, 1H), 4.04 (d, *J* = 6.2 Hz, 2H), 1.73 – 1.57 (m, 6H), 1.25 – 1.13 (m, 2H), 1.12 – 1.03 (m, 1H), 0.99 – 0.89 (m, 2H).

*4.1.6.12. Synthesis of 4-(benzyloxy)-3-(1H-tetrazol-1-yl) benzimidamide hydrochloride (**6l**)*

A white solid, yield: 46.4%. MS (ESI) m/z: 295.2 $[M + H]^+$; ^{1}H NMR (600 MHz, DMSO-d_6) δ 9.91 (s, 1H), 8.86 (s, 4H), 8.29 (d, *J* = 2.4 Hz, 1H), 8.14 (dd, *J* = 8.9, 2.5 Hz, 1H), 7.68 (d, *J* = 9.0 Hz, 1H), 7.42 – 7.36 (m, 4H), 7.36 – 7.32 (m, 1H), 5.39 (s, 2H).

*4.1.6.13. Synthesis of 4-[(4-methylbenzyl) oxy]-3-(1H-tetrazol-1-yl) benzimidamide hydrochloride (**6m**)*

A white solid, yield: 42.5%. MS (ESI) m/z: 309.4 $[M + H]^+$; 307.3 $[M - H]^-$; ^{1}H NMR (600 MHz, DMSO-d_6) δ 9.89 (s, 1H), 8.92 (s, 4H), 8.28 (d, *J* = 2.4 Hz, 1H), 8.13 (dd, *J* = 8.9, 2.5 Hz, 1H), 7.67 (d, *J* = 8.9 Hz, 1H), 7.29 (d, *J* = 7.8 Hz, 2H), 7.19 (d, *J* = 7.7 Hz, 2H), 5.34 (s, 2H), 2.29 (s, 3H).

*4.1.6.14. Synthesis of 4-{[4-(tert-butyl) benzyl] oxy}-3-(1H-tetrazol-1-yl) benzimidamide hydrochloride (**6n**)*

A white solid, yield: 46.1%. MS (ESI) m/z: 351.3 $[M + H]^+$; 349.4 $[M - H]^-$; ^{1}H NMR (600 MHz, DMSO-d_6) δ 9.92 (s, 1H), 8.30 (d, *J* = 2.4 Hz, 1H), 8.16 (dd, *J* = 8.9, 2.4 Hz, 1H), 7.70 (d, *J* = 9.0 Hz, 1H), 7.43 – 7.37 (m,

2H), 7.36 – 7.29 (m, 2H), 5.35 (s, 2H), 1.26 (s, 9H).

*4.1.6.15. Synthesis of 4-[(4-methoxybenzyl) oxy]-3-(1H-tetrazol-1-yl) benzimidamide hydrochloride (**6o**)*

A white solid, yield: 74.6%. MS (ESI) m/z: 325.2 $[M + H]^+$; 323.0 $[M - H]^-$; ^{1}H NMR (600 MHz, DMSO-d_6) δ 9.93 (s, 1H), 8.36 (d, *J* = 2.4 Hz, 1H), 8.24 (dd, *J* = 8.9, 2.4 Hz, 1H), 8.10 (s, 15H), 7.73 (d, *J* = 9.0 Hz, 1H), 7.37 (dd, 2H), 6.94 (dd, 2H), 5.32 (s, 2H), 3.75 (s, 3H).

*4.1.6.16. Synthesis of 4-[(4-fluorobenzyl) oxy]-3-(1H-tetrazol-1-yl) benzimidamide hydrochloride (**6p**)*

A white solid, yield: 38.6%. MS (ESI) m/z: 313.2 $[M + H]^+$; 311.3 $[M - H]^-$; ^{1}H NMR (600 MHz, DMSO-d_6) δ 9.93 (s, 1H), 8.97 (s, 6H), 8.32 (s, 1H), 8.19 (dd, *J* = 9.0, 2.4 Hz, 1H), 7.69 (d, *J* = 8.9 Hz, 1H), 7.48 (dd, *J* = 8.4, 5.4 Hz, 2H), 7.29 – 7.13 (m, 2H), 5.38 (s, 2H).

*4.1.6.17. Synthesis of 4-[(4-chlorobenzyl) oxy]-3-(1H-tetrazol-1-yl) benzimidamide hydrochloride (**6q**)*

A white solid, yield: 39.0%. MS (ESI) m/z: 329.1 $[M + H]^+$; 327.1 $[M - H]^-$; ^{1}H NMR (600 MHz, DMSO-d_6) δ 9.93 (s, 1H), 9.37 (s, 5H), 8.31 (d, *J* = 2.2 Hz, 1H), 8.16 (dd, *J* = 9.0, 2.4 Hz, 1H), 7.67 (d, *J* = 8.9 Hz, 1H), 7.45 (dd, *J* = 2.3 Hz, 4H), 5.39 (s, 2H).

*4.1.6.18. Synthesis of 4-[(4-bromobenzyl) oxy]-3-(1H-tetrazol-1-yl) benzimidamide hydrochloride (**6r**)*

A white solid, yield: 34.6%. MS (ESI) m/z: 373.1 $[M + H]^+$; 395.2 $[M + Na]^+$; ^{1}H NMR (600 MHz, DMSO-d_6) δ 9.94 (s, 1H), 9.47 (s, 4H), 8.32 (s, 1H), 8.17 (d, *J* = 8.9 Hz, 1H), 7.67 (d, *J* = 8.9 Hz, 1H), 7.59 (d, *J* = 7.9 Hz, 2H), 7.38 (d, *J* = 8.0 Hz, 2H), 5.38 (s, 2H).

*4.1.6.19. Synthesis of 4-[(3-methoxybenzyl) oxy]-3-(1H-tetrazol-1-yl) benzimidamide hydrochloride (**6s**)*

A white solid, yield: 34.6%. MS (ESI) m/z: 325.2 $[M + H]^+$; 347.2 $[M + Na]^+$; 323.0 $[M - H]^-$; ^{1}H NMR (400 MHz, DMSO-d_6) δ 9.97 (s, 1H), 8.36 (d, *J* = 2.3 Hz, 1H), 8.23 (dd, 1H), 8.12 (s, 8H), 7.67 (d, *J* = 8.9 Hz, 1H), 7.28 (t, *J* = 7.8 Hz, 1H), 7.01 – 6.92 (m, 2H), 6.88 (dd, *J* = 8.3, 2.5 Hz, 1H), 5.36 (s, 2H).

*4.1.6.20. Synthesis of 4-[(3-fluorobenzyl) oxy]-3-(1H-tetrazol-1-yl) benzimidamide hydrochloride (**6t**)*

A white solid, yield: 66.3%. MS (ESI) m/z: 313.2 $[M + H]^+$; 335.2 $[M + Na]^+$; 311.0 $[M - H]^-$; ^{1}H NMR (400 MHz, DMSO-d_6) δ 9.98 (s, 1H), 8.36 (d, *J* = 2.4 Hz, 1H), 8.22 (dd, *J* = 8.9, 2.4 Hz, 1H), 7.95 (s, 16H), 7.67 (d, *J*

= 8.9 Hz, 1H), 7.48 – 7.39 (m, 1H), 7.30 – 7.21 (m, 2H), 7.20 – 7.12 (m, 1H), 5.41 (s, 2H).

*4.1.6.21. Synthesis of 4-[(3-chlorobenzyl) oxy]-3-(1H-tetrazol-1-yl) benzimidamide hydrochloride (**6u**)*

A white solid, yield: 26.7%. MS (ESI) m/z: 329.2 $[M + H]^+$; 327.0 $[M - H]^-$; ^{1}H NMR (600 MHz, DMSO-d_6) δ 10.00 (s, 1H), 8.37 (s, 1H), 8.24 (d, *J* = 8.8 Hz, 1H), 7.67 (s, 59H), 7.48 (s, 1H), 7.43 – 7.33 (m, 3H), 5.40 (s, 2H).

*4.1.6.22. Synthesis of 4-[(3-bromobenzyl) oxy]-3-(1H-tetrazol-1-yl) benzimidamide hydrochloride (**6v**)*

A white solid, yield: 64.1%. MS (ESI) m/z: 373.3 $[M + H]^+$; 370.9 $[M - H]^-$; ^{1}H NMR (600 MHz, DMSO-d_6) δ 9.98 (s, 1H), 8.36 (d, *J* = 2.4 Hz, 1H), 8.22 (dd, *J* = 8.9, 2.5 Hz, 1H), 8.09 (s, 8H), 7.66 (d, *J* = 9.0 Hz, 1H), 7.62 (s, 1H), 7.34 (t, *J* = 7.8 Hz, 1H), 5.40 (s, 2H).

*4.1.6.23. Synthesis of 4-[(2-chlorobenzyl) oxy]-3-(1H-tetrazol-1-yl) benzimidamide hydrochloride (**6w**)*

A white solid, yield: 43.1%. MS (ESI) m/z: 329.3 $[M + H]^+$; 351.3 $[M + Na]^+$; 327.1 $[M - H]^-$; ^{1}H NMR (400 MHz, DMSO-d_6) δ 9.86 (s, 1H), 8.43 (s, 1H), 8.35 (d, *J* = 2.3 Hz, 1H), 8.26 (s, 10H), 7.75 (d, *J* = 8.9 Hz, 1H), 7.53 – 7.46 (m, 2H), 7.43 – 7.32 (m, 2H), 5.44 (s, 2H).

*4.1.6.24. Synthesis of 4-[(2, 6-dichlorobenzyl) oxy]-3-(1H-tetrazol-1-yl) benzimidamide hydrochloride (**6x**)*

A white solid, yield: 39.8%. MS (ESI) m/z: 363.1 $[M + H]^+$.

*4.1.6.25. Synthesis of 4-[(2, 4-dichlorobenzyl) oxy]-3-(1H-tetrazol-1-yl) benzimidamide hydrochloride (**6y**)*

A white solid, yield: 36.4%. MS (ESI) m/z: 363.0 $[M - H]^-$; 1H NMR (400 MHz, DMSO-d6) δ 9.90 (s, 1H), 8.43 (s, 1H), 8.39 (d, *J* = 2.3 Hz, 1H), 8.28 (d, *J* = 6.5 Hz, 1H), 7.86 (s, 12H), 7.69 (s, 1H), 7.57 (d, *J* = 8.3 Hz, 1H), 7.48 (d, *J* = 7.9 Hz, 1H), 5.45 (s, 2H).

*4.1.7. General procedure for synthesis of ethyl 2-[4-alkoxy-3-(1H-tetrazol-1-yl) phenyl]-6-oxo-1, 6-dihydropyrimidine-5-carboxylates (**7a-7y**)*

To a solution of sodium hydride (3 g, 0.125 mol) in ethanol (10 mL) were added compounds **7a-7y** (1.97 mmol) and diethyl ethoxymethylenemalonate (460 mg, 2.16 mmol). The reaction mixture was stirred at room temperature until the material spot disapperaed by TLC. After the reaction completed, the mixture was added 5

mL 6 M hydrochloric acid and stirred for 0.5 h, then the precipitate was collected by filtration. The resulting residue was refluxed (ethanol or ethanol: dechloromethane=1:1) to yield ethyl 2-[4-alkoxy-3-(1*H*-tetrazol-1-yl) phenyl]-6-oxo-1, 6-dihydropyrimidine-5-carboxylates (**7a-7y**).

*4.1.7.1. Synthesis of ethyl 2-[4-methoxy-3-(1H-tetrazol-1-yl) phenyl]-6-oxo-1, 6-dihydropyrimidine-5-carboxylate (**7a**)*

A white solid, yield: 48.6%. Mp: degraded at 216.7°C. MS (ESI) m/z: 341.1 $[M - H]^-$; ^{1}H NMR (600 MHz, DMSO-d_6) δ 13.22 (s, 1H), 9.87 (s, 1H), 8.64 (s, 1H), 8.57 (s, 1H), 8.45 (d, *J* = 8.2 Hz, 1H), 7.55 (d, *J* = 8.9 Hz, 1H), 4.25 (q, *J* = 7.0 Hz, 2H), 3.98 (s, 3H), 1.28 (t, *J* = 7.0 Hz, 3H).

*4.1.7.2. Synthesis of ethyl 2-[4-isopropoxy-3-(1H-tetrazol-1-yl) phenyl]-6-oxo-1, 6-dihydropyrimidine-5-carboxylate (**7b**)*

A white solid, yield: 48.4%. Mp 183.1°C-184.5°C. MS (ESI) m/z: 369.2 $[M - H]^-$; ^{1}H NMR (600 MHz, DMSO-d_6) δ 13.23 (s, 1H), 9.81 (s, 1H), 8.65 (s, 1H), 8.58 (s, 1H), 8.43 (d, *J* = 9.0 Hz, 1H), 7.58 (d, *J* = 9.0 Hz, 1H), 4.94 (hept, *J* = 6.0 Hz, 1H), 4.26 (q, *J* = 7.1 Hz, 2H), 1.30 (d, *J* = 6.0 Hz, 6H), 1.28 (t, *J* = 7.1 Hz, 2H).

*4.1.7.3. Synthesis of ethyl 2-[4-isobutoxy-3-(1H-tetrazol-1-yl) phenyl]-6-oxo-1, 6-dihydropyrimidine-5-carboxylate (**7c**)*

A white solid, yield: 70.1%. Mp 204.1°C-204.7°C. MS (ESI) m/z: 385.4 $[M + H]^+$; 407.3 $[M + Na]^+$; 383.2 $[M - H]^-$; ^{1}H NMR (600 MHz, DMSO-d_6) δ 13.20 (s, 1H), 9.81 (s, 1H), 8.64 (s, 1H), 8.55 (d, *J* = 2.0 Hz, 1H), 8.44 (dd, *J* = 8.9, 2.4 Hz, 1H), 7.54 (d, *J* = 9.0 Hz, 1H), 4.25 (q, *J* = 7.1 Hz, 2H), 4.00 (d, *J* = 6.4 Hz, 2H), 1.99 (hept, *J* = 6.6 Hz, 1H), 1.28 (t, *J* = 7.1 Hz, 3H), 0.87 (d, *J* = 6.7 Hz, 6H).

*4.1.7.4. Synthesis of ethyl 2-[4-(isopentyloxy)-3-(1H-tetrazol-1-yl) phenyl]-6-oxo-1, 6-dihydropyrimidine-5-carboxylate (**7d**)*

A white solid, yield: 40.2%. Mp 204.3°C-204.8°C. MS (ESI) m/z: 399.3 $[M + H]^+$; 421.2 $[M + Na]^+$; 437.2 $[M + K]^+$; 397.0 $[M - H]^-$; ^{1}H NMR (600 MHz, DMSO-d_6) δ 13.21 (s, 1H), 9.80 (s, 1H), 8.63 (s, 1H), 8.55 (s, 1H), 8.43 (d, *J* = 7.8 Hz, 1H), 7.56 (d, *J* = 9.0 Hz, 1H), 4.29 – 4.20 (m, 4H), 1.65 – 1.57 (m, 3H), 1.28 (t, *J* = 7.1 Hz, 3H), 0.86 (d, *J* = 6.1 Hz, 6H).

*4.1.7.5. Synthesis of ethyl 2-[4-(allyloxy)-3-(1H-tetrazol-1-yl) phenyl]-6-oxo-1, 6-dihydropyrimidine-5-carboxylate (**7e**)*

A white solid, yield: 69.8%. Mp: degraded at 231.2°C. MS (ESI) m/z: 369.3 $[M + H]^+$; 391.2 $[M + Na]^+$; 407.2 $[M + K]^+$; 367.0 $[M - H]^-$; ^{1}H NMR (600 MHz, DMSO-d_6) δ 9.85 (s, 1H), 8.56 (s, 1H), 8.52 (s, 1H), 8.48 (d, *J* = 8.6 Hz, 1H), 7.37 (d, *J* = 8.7 Hz, 1H), 6.00 (ddt, *J* = 16.3, 10.5, 5.1 Hz, 1H), 5.26 (dd, *J* = 25.2, 13.9 Hz, 2H), 4.74 (d, *J* = 5.1 Hz, 2H), 4.16 (q, *J* = 7.1 Hz, 2H), 1.25 (t, *J* = 6.7 Hz, 3H).

*4.1.7.6. Synthesis of ethyl 2-{4-[(2-methylallyl) oxy]-3-(1H-tetrazol-1-yl) phenyl}-6-oxo-1, 6-dihydropyrimidine-5-carboxylate (**7f**)*

A white solid, yield: 61.4%. Mp: degraded at 219.8°C. MS (ESI) m/z: 405.4 $[M + Na]^+$; 381.1 $[M - H]^-$; ^{1}H NMR (600 MHz, DMSO-d_6) δ 13.22 (s, 1H), 9.84 (s, 1H), 8.64 (s, 1H), 8.55 (s, 1H), 8.44 (d, *J* = 8.9 Hz, 1H), 7.55 (d, *J* = 9.0 Hz, 1H), 4.95 (d, *J* = 8.4 Hz, 2H), 4.73 (s, 2H), 4.26 (q, *J* = 7.1 Hz, 2H), 1.68 (s, 3H), 1.28 (t, *J* = 7.1 Hz, 3H).

*4.1.7.7. Synthesis of ethyl 2-{4-[(3-methylbut-2-en-1-yl) oxy]-3-(1H-tetrazol-1-yl) phenyl}-6-oxo-1, 6-dihydropyrimidine-5-carboxylate (**7g**)*

A white solid, yield: 63.4%. Mp 204.2°C-204.5°C. MS (ESI) m/z: 397.4 $[M + H]^+$; 419.3 $[M + Na]^+$; 395.1 $[M - H]^-$; ^{1}H NMR (600 MHz, DMSO-d_6) δ 13.21 (s, 1H), 9.81 (s, 1H), 8.65 (s, 1H), 8.56 (d, *J* = 1.8 Hz, 1H), 8.44 (dd, *J* = 8.9, 2.4 Hz, 1H), 7.57 (d, *J* = 9.0 Hz, 1H), 5.41 (t, *J* = 6.5 Hz, 1H), 4.80 (d, *J* = 6.6 Hz, 2H), 4.26 (q, *J* = 7.1 Hz, 2H), 1.73 (s, 3H), 1.69 (s, 3H), 1.28 (t, *J* = 7.1 Hz, 3H).

*4.1.7.8. Synthesis of ethyl 6-oxo-2-[4-(prop-2-yn-1-yloxy)-3-(1H-tetrazol-1-yl) phenyl]-1, 6-dihydropyrimidine-5-carboxylate (**7h**)*

A white solid, yield: 55.6%. Mp 211.3°C-212.0°C. MS (ESI) m/z: 365.0 $[M - H]^-$; ^{1}H NMR (400 MHz, DMSO-d_6) δ 13.22 (s, 1H), 9.84 (s, 1H), 8.66 (s, 1H), 8.58 (d, *J* = 2.3 Hz, 1H), 8.47 (dd, *J* = 9.0, 2.3 Hz, 1H), 7.61 (d, *J* = 9.0 Hz, 1H), 5.09 (d, *J* = 2.4 Hz, 2H), 4.26 (q, *J* = 7.1 Hz, 2H), 3.73 (t, *J* = 2.4 Hz, 1H), 1.29 (t, *J* = 7.1 Hz, 3H).

*4.1.7.9. Synthesis of ethyl 2-[4-(cyclopropylmethoxy)-3-(1H-tetrazol-1-yl) phenyl]-6-oxo-1, 6-dihydropyrimidine-5-carboxylate (**7i**)*

A white solid, yield: 58.4%. Mp: degraded at 210.1°C. MS (ESI) m/z: 405.4 $[M + Na]^+$; 381.3 $[M - H]^-$; ^{1}H

NMR (400 MHz, DMSO-d_6) δ 13.26 (s, 1H), 9.86 (s, 1H), 8.63 (s, 1H), 8.59 (d, *J* = 2.3 Hz, 1H), 8.44 (dd, *J* = 8.9, 2.3 Hz, 1H), 7.53 (d, *J* = 8.9 Hz, 1H), 4.26 (q, *J* = 7.1 Hz, 2H), 4.12 (d, *J* = 7.0 Hz, 2H), 1.29 (t, *J* = 7.1 Hz, 3H), 0.55 (dt, 2H), 0.34 (dt, *J* = 6.2, 4.3 Hz, 2H).

*4.1.7.10. Synthesis of ethyl 2-[4-(cyclopentyloxy)-3-(1H-tetrazol-1-yl) phenyl]-6-oxo-1, 6-dihydropyrimidine-5-carboxylate (**7J**)*

A white solid, yield: 67.0%. Mp: degraded at 204.5°C. MS (ESI) m/z: 419.3 $[M + Na]^+$; 395.1 $[M - H]^-$; ^1H NMR (600 MHz, DMSO-d_6) δ 13.21 (s, 1H), 9.77 (s, 1H), 8.64 (s, 1H), 8.56 (s, 1H), 8.43 (d, *J* = 8.8 Hz, 1H), 7.55 (d, *J* = 8.9 Hz, 1H), 5.14 (p, 1H), 4.25 (q, *J* = 7.1 Hz, 2H), 1.98 – 1.88 (m, 2H), 1.76 – 1.68 (m, 2H), 1.57 (q, *J* = 4.9, 3.4 Hz, 4H), 1.28 (t, *J* = 7.1 Hz, 3H) .

*4.1.7.11. Synthesis of ethyl 2-[4-(cyclohexylmethoxy)-3-(1H-tetrazol-1-yl) phenyl]-6-oxo-1, 6-dihydropyrimidine-5-carboxylate (**7k**)*

A white solid, yield: 47.8%. Mp: degraded at 190.8°C. MS (ESI) m/z: 405.4 $[M + Na]^+$; 381.3 $[M - H]^-$; ^1H NMR (600 MHz, DMSO-d_6) δ 13.23 (s, 1H), 9.80 (s, 1H), 8.64 (s, 1H), 8.55 (d, *J* = 2.3 Hz, 1H), 8.45 (dd, 1H), 7.55 (d, *J* = 9.0 Hz, 1H), 4.25 (q, *J* = 7.1 Hz, 2H), 4.03 (d, *J* = 6.3 Hz, 2H), 1.75 – 1.58 (m, 6H), 1.28 (t, *J* = 7.1 Hz, 3H), 1.24 – 1.14 (m, 3H), 1.13 – 1.04 (m, 1H), 0.98 – 0.89 (m, 2H) .

*4.1.7.12. Synthesis of ethyl 2-[4-(benzyloxy)-3-(1H-tetrazol-1-yl) phenyl]-6-oxo-1, 6-dihydropyrimidine-5-carboxylate (**7l**)*

A white solid, yield: 69.6%. Mp: degraded at 216.9°C. MS (ESI) m/z: 419.2 $[M + H]^+$; 441.1 $[M + Na]^+$; 417.0 $[M - H]^-$; ^1H NMR (600 MHz, DMSO-d_6) δ 13.21 (s, 1H), 9.85 (s, 1H), 8.64 (s, 1H), 8.58 (d, *J* = 1.9 Hz, 1H), 8.44 (dd, *J* = 9.0, 2.3 Hz, 1H), 7.63 (d, *J* = 9.0 Hz, 1H), 7.43 – 7.37 (m, 4H), 7.36 – 7.32 (m, 1H), 5.37 (s, 2H), 4.25 (q, *J* = 7.1 Hz, 2H), 1.28 (t, *J* = 7.1 Hz, 3H) .

*4.1.7.13. Synthesis of ethyl 2-{4-[(4-methylbenzyl) oxy]-3-(1H-tetrazol-1-yl) phenyl}-6-oxo-1, 6-dihydropyrimidine-5-carboxylate (**7m**)*

A white solid, yield: 72.1%. Mp: degraded at 225.3°C. MS (ESI) m/z: 431.1 $[M - H]^-$; ^1H NMR (600 MHz, DMSO-d_6) δ 13.22 (s, 1H), 9.82 (s, 1H), 8.64 (s, 1H), 8.57 (s, 1H), 8.43 (d, *J* = 8.0 Hz, 1H), 7.63 (d, *J* = 9.0 Hz, 1H), 7.30 (d, *J* = 7.9 Hz, 2H), 7.19 (d, *J* = 7.9 Hz, 2H), 5.32 (s, 2H), 4.25 (q, *J* = 7.1 Hz, 2H), 2.29 (s, 3H), 1.28

(t, *J* = 7.1 Hz, 3H).

*4.1.7.14. Synthesis of ethyl 2-{4-{[4-(tert-butyl) benzyl] oxy}-3-(1H-tetrazol-1-yl) phenyl}-6-oxo-1, 6-dihydropyrimidine-5-carboxylate (**7n**)*

A white solid, yield: 68.3%. Mp: degraded at 225.5°C. MS (ESI) m/z: 475.2 $[M + H]^+$; 497.2 $[M + Na]^+$; 513.2 $[M + K]^+$; 473.1 $[M - H]^-$; ^{1}H NMR (600 MHz, DMSO-d_6) δ 13.21 (s, 1H), 9.85 (s, 1H), 8.64 (s, 1H), 8.57 (d, *J* = 2.3 Hz, 1H), 8.44 (dd, *J* = 8.9, 2.4 Hz, 1H), 7.65 (d, *J* = 9.0 Hz, 1H), 7.40 (d, *J* = 8.4 Hz, 2H), 7.33 (d, *J* = 8.3 Hz, 2H), 5.33 (s, 2H), 4.25 (q, *J* = 7.1 Hz, 2H), 1.29 (t, *J* = 7.1 Hz, 3H), 1.26 (s, 9H) .

*4.1.7.15. Synthesis of ethyl 2-{4-[(4-methoxybenzyl) oxy]-3-(1H-tetrazol-1-yl) phenyl}-6-oxo-1, 6-dihydropyrimidine-5-carboxylate (**7o**)*

A white solid, yield: 50.6%. Mp: degraded at 208.4°C. MS (ESI) m/z: 471.3 $[M + Na]^+$; 447.0 $[M - H]^-$; ^{1}H NMR (400 MHz, DMSO-d_6) δ 13.21 (s, 1H), 9.80 (s, 1H), 8.64 (s, 1H), 8.57 (d, *J* = 2.3 Hz, 1H), 8.45 (dd, *J* = 8.8, 2.3 Hz, 1H), 7.66 (d, *J* = 9.0 Hz, 1H), 7.36 (dd, 2H), 6.94 (dd, 2H), 5.29 (s, 2H), 4.26 (q, *J* = 7.1 Hz, 2H), 3.75 (s, 3H), 1.29 (t, *J* = 7.1 Hz, 3H).

*4.1.7.16. Synthesis of ethyl 2-{4-[(4-fluorobenzyl) oxy]-3-(1H-tetrazol-1-yl) phenyl}-6-oxo-1, 6-dihydropyrimidine-5-carboxylate (**7p**)*

A white solid, yield: 39.3%. Mp: degraded at 180.0°C. MS (ESI) m/z: 459.4 $[M + Na]^+$; 435.2 $[M - H]^-$; ^{1}H NMR (400 MHz, DMSO-d_6) δ 9.82 (s, 1H), 8.53 (s, 1H), 8.52 (d, *J* = 1.8 Hz, 1H), 8.49 (dd, *J* = 8.7, 2.1 Hz, 1H), 7.51 – 7.41 (m, 3H), 7.26 – 7.17 (m, 2H), 5.27 (s, 2H), 4.16 (q, *J* = 7.1 Hz, 2H), 1.25 (t, *J* = 7.1 Hz, 3H).

*4.1.7.17. Synthesis of ethyl 2-{4-[(4-chlorobenzyl) oxy]-3-(1H-tetrazol-1-yl) phenyl}-6-oxo-1, 6-dihydropyrimidine-5-carboxylate (**7q**)*

A white solid, yield: 30.1%. Mp: degraded at 230.4°C. MS (ESI) m/z: 475.4 $[M + Na]^+$; ^{1}H NMR (400 MHz, DMSO-d_6) δ 13.21 (s, 1H), 9.85 (s, 1H), 8.65 (s, 1H), 8.58 (d, *J* = 2.3 Hz, 1H), 8.51 – 8.39 (m, 1H), 7.62 (d, *J* = 9.0 Hz, 1H), 7.53 – 7.38 (m, 4H), 5.37 (s, 2H), 4.26 (q, *J* = 7.1 Hz, 2H), 1.28 (t, *J* = 7.1 Hz, 3H).

*4.1.7.18. Synthesis of ethyl 2-{4-[(4-bromobenzyl) oxy]-3-(1H-tetrazol-1-yl) phenyl}-6-oxo-1, 6-dihydropyrimidine-5-carboxylate (**7r**)*

An off white solid, yield: 55.2%. Mp: degraded at 229.5°C. MS (ESI) m/z: 519.4 $[M + Na]^+$; 495.2 $[M - H]^-$; ^{1}H NMR (600 MHz, DMSO-d_6) δ 9.84 (s, 1H), 8.52 (s, 1H), 8.52 (d, *J* = 2.0 Hz, 1H), 8.48 (dd, *J* = 8.8, 2.1 Hz, 1H), 7.58 (d, *J* = 8.1 Hz, 2H), 7.46 (d, *J* = 8.8 Hz, 1H), 7.35 (d, *J* = 8.0 Hz, 2H), 5.27 (s, 2H), 4.16 (q, *J* = 7.1 Hz, 2H), 1.25 (t, *J* = 7.0 Hz, 3H).

*4.1.7.19. Synthesis of ethyl 2-{4-[(3-methoxybenzyl) oxy]-3-(1H-tetrazol-1-yl) phenyl}-6-oxo-1, 6-dihydropyrimidine-5-carboxylate (**7s**)*

A white solid, yield: 61.8%. Mp: degraded at 209.9°C. MS (ESI) m/z: 449.4 $[M + H]^+$; 471.2 $[M + Na]^+$; 447.1 $[M - H]^-$; ^{1}H NMR (600 MHz, DMSO-d_6) δ 13.23 (s, 1H), 9.88 (s, 1H), 8.65 (s, 1H), 8.58 (s, 1H), 8.45 (d, *J* = 8.8 Hz, 1H), 7.63 (d, *J* = 9.0 Hz, 1H), 7.29 (t, *J* = 7.9 Hz, 1H), 6.95 (d, *J* = 6.8 Hz, 2H), 6.92 – 6.85 (m, 1H), 5.35 (s, 2H), 4.26 (q, *J* = 7.0 Hz, 2H), 3.74 (s, 3H), 1.28 (t, *J* = 7.1 Hz, 3H).

*4.1.7.20. Synthesis of ethyl 2-{4-[(3-fluorobenzyl) oxy]-3-(1H-tetrazol-1-yl) phenyl}-6-oxo-1, 6-dihydropyrimidine-5-carboxylate (**7t**)*

A white solid, yield: 46.8%. Mp: degraded at 214.9°C. MS (ESI) m/z: 437.4 $[M + H]^+$; 459.3 $[M + Na]^+$; 435.1 $[M - H]^-$; ^{1}H NMR (400 MHz, DMSO-d_6) δ 13.21 (s, 1H), 9.89 (s, 1H), 8.65 (s, 1H), 8.58 (s, 1H), 8.45 (d, *J* = 8.9 Hz, 1H), 7.62 (d, *J* = 9.0 Hz, 1H), 7.44 (dd, *J* = 7.4 Hz, 1H), 7.24 (d, *J* = 8.3 Hz, 2H), 7.18 (t, *J* = 8.5 Hz, 1H), 5.40 (s, 2H), 4.26 (q, *J* = 7.1 Hz, 2H), 1.29 (t, *J* = 7.1 Hz, 3H).

*4.1.7.21. Synthesis of ethyl 2-{4-[(3-chlorobenzyl) oxy]-3-(1H-tetrazol-1-yl) phenyl}-6-oxo-1, 6-dihydropyrimidine-5-carboxylate (**7u**)*

A white solid, yield: 49.3%. Mp 209.4°C-209.6°C. MS (ESI) m/z: 453.2 $[M + H]^+$; 475.2 $[M + Na]^+$; 451.0 $[M - H]^-$; ^{1}H NMR (600 MHz, DMSO-d_6) δ 13.23 (s, 0H), 9.90 (s, 1H), 8.65 (s, 0H), 8.58 (s, 1H), 8.45 (d, *J* = 8.9 Hz, 1H), 7.62 (d, *J* = 9.0 Hz, 1H), 7.49 (s, 1H), 7.46 – 7.38 (m, 3H), 7.36 (d, *J* = 6.8 Hz, 1H), 5.39 (s, 2H), 4.26 (q, *J* = 7.0 Hz, 2H), 1.28 (t, *J* = 7.1 Hz, 3H).

*4.1.7.22. Synthesis of ethyl 2-{4-[(3-bromobenzyl) oxy]-3-(1H-tetrazol-1-yl) phenyl}-6-oxo-1, 6-dihydropyrimidine-5-carboxylate (**7v**)*

A white solid, yield: 51.4%. Mp 211.0°C -211.2°C. MS (ESI) m/z: 519.1 $[M + Na]^+$; 495.0 $[M - H]^-$; ^{1}H NMR (400 MHz, DMSO-d_6) δ 13.19 (s, 1H), 9.88 (s, 1H), 8.64 (s, 1H), 8.58 (d, *J* = 2.3 Hz, 1H), 8.44 (dd, *J* =

8.8, 2.3 Hz, 1H), 7.64 – 7.58 (m, 2H), 7.57 – 7.50 (m, 1H), 7.43 – 7.33 (m, 2H), 5.37 (s, 2H), 4.25 (q, *J* = 7.1 Hz, 2H), 1.28 (t, *J* = 7.1 Hz, 3H).

*4.1.7.23. Synthesis of ethyl 2-{4-[(2-chlorobenzyl) oxy]-3-(1H-tetrazol-1-yl) phenyl}-6-oxo-1, 6-dihydropyrimidine-5-carboxylate (**7w**)*

A white solid, yield: 63.2%. Mp: degraded at 209.0°C. MS (ESI) m/z: 453.4 $[M + H]^+$; 475.4 $[M + Na]^+$; 451.3 $[M - H]^-$; ^{1}H NMR (400 MHz, DMSO-d_6) δ 13.21 (s, 1H), 9.77 (s, 1H), 8.65 (s, 1H), 8.58 (d, *J* = 2.2 Hz, 1H), 8.47 (dd, *J* = 8.9, 2.3 Hz, 1H), 7.70 (d, *J* = 8.9 Hz, 1H), 7.54 – 7.46 (m, 2H), 7.44 – 7.33 (m, 2H), 5.43 (s, 2H), 4.26 (q, *J* = 7.1 Hz, 2H), 1.29 (t, *J* = 7.1 Hz, 3H).

*4.1.7.24. Synthesis of ethyl 2-{4-[(2, 6-dichlorobenzyl) oxy]-3-(1H-tetrazol-1-yl) phenyl}-6-oxo-1, 6-dihydropyrimidine-5-carboxylate (**7x**)*

A white solid, yield: 47.9%. Mp: degraded at 229.1°C. MS (ESI) m/z: 510.3 $[M + Na]^+$; 486.3 $[M - H]^-$; ^{1}H NMR (400 MHz, DMSO-d_6) δ 13.28 (s, 1H), 9.57 (s, 1H), 8.66 (s, 1H), 8.57 (d, *J* = 2.3 Hz, 1H), 8.53 (dd, *J* = 8.8, 2.4 Hz, 1H), 7.87 (d, *J* = 8.9 Hz, 1H), 7.58 – 7.52 (m, 2H), 7.46 (dd, *J* = 9.1, 6.9 Hz, 1H), 5.50 (s, 2H), 4.26 (q, *J* = 7.1 Hz, 2H), 1.29 (t, *J* = 7.1 Hz, 3H).

*4.1.7.25. Synthesis of ethyl 2-{4-[(2, 4-dichlorobenzyl) oxy]-3-(1H-tetrazol-1-yl) phenyl}-6-oxo-1, 6-dihydropyrimidine-5-carboxylate (**7y**)*

A white solid, yield: 56.7%. Mp: degraded at 237.0°C. MS (ESI) m/z: 509.0 $[M + Na]^+$; ^{1}H NMR (400 MHz, DMSO-d_6) δ 13.30 (s, 1H), 9.80 (s, 1H), 8.64 (s, 1H), 8.58 (d, *J* = 2.3 Hz, 1H), 8.53 – 8.45 (m, 1H), 7.71 (d, *J* = 9.0 Hz, 1H), 7.69 (d, *J* = 2.1 Hz, 1H), 7.53 (d, *J* = 8.3 Hz, 1H), 7.47 (dd, *J* = 8.3, 2.1 Hz, 1H), 5.42 (s, 2H), 4.26 (q, *J* = 7.1 Hz, 2H), 1.28 (t, *J* = 7.1 Hz, 3H).

*4.1.8. General procedure for synthesis of 2-[4-alkoxy-3-(1H-tetrazol-1-yl) phenyl]-6-oxo-1, 6-dihydropyrimidine-5-carboxylic acids (**8a-8y**)*

A mixture of ethyl 2-[4-alkoxy-3-(1*H*-tetrazol-1-yl) phenyl]-6-oxo-1,6-dihydropyrimidine-5- carboxylates **7a-7y** (1.46 mmol) , 10% LiOH aqueous (5 mL) and THF (10 mL) were stirred at 50°C until the material spot disapperaed by TLC. The solvent was concentrated in a vacuum, and the residue was acidified with dilute hydrochloric acid to pH 1. The resulting precipitate was filtered , and refluxed for 0.5 h with a mixture of THF

and H_2O (2:1) to yield the corresponding 2-[4-alkoxy-3-(1*H*-tetrazol-1-yl) phenyl]-6-oxo-1, 6-dihydropyrimidine-5-carboxylic acids (**8a-8y**).

*4.1.8.1. Synthesis of 2-[4-methoxy-3-(1H-tetrazol-1-yl) phenyl]-6-oxo-1, 6-dihydropyrimidine-5-carboxylic acid (**8a**)*

A white solid, yield: 76.3%. Mp: degraded at 181.7°C. ESI-HRMS calcd. for $C_{13}H_9N_6O_4$ $[M - H]^-$ 313.0691, found: 313.0781; ^{1}H NMR (600 MHz, DMSO-d_6) δ 9.89 (s, 1H), 8.72 (s, 1H), 8.58 (d, *J* = 2.1 Hz, 1H), 8.47 (dd, *J* = 8.9, 2.0 Hz, 1H), 7.59 (d, *J* = 8.9 Hz, 1H), 3.99 (s, 3H). ^{13}C NMR (100 MHz, DMSO-d_6) δ 165.30 , 159.70 , 155.56 , 145.20 , 145.20 , 145.19 , 132.38 , 126.44 , 124.92 , 123.21 , 114.04 , 111.57 , 57.52 . IR (KBr, cm^{-1}) 3470.2, 3111.7, 2847.0, 1725.2, 1480.7, 1293.6.

*4.1.8.2. Synthesis of 2-[4-isopropoxy-3-(1H-tetrazol-1-yl)phenyl]-6-oxo-1,6-dihydropyrimidine-5-carboxylic acid (**8b**)*

A white solid, yield: 80.1%. Mp: degraded at 232.0°C . ESI-HRMS calcd. for $C_{15}H_{13}N_6O_4$ $[M - H]^-$ 341.1004, found: 341.1135; ^{1}H NMR (600 MHz, DMSO-d_6) δ 9.83 (s, 1H), 8.73 (s, 1H), 8.57 (s, 1H), 8.43 (dd, *J* = 8.8, 2.4 Hz, 1H), 7.62 (d, *J* = 9.1 Hz, 1H), 4.95 (hept, *J* = 6.0 Hz, 1H), 1.31 (d, *J* = 6.0 Hz, 7H) .^{13}C NMR (100 MHz, DMSO-d_6) δ 164.99 , 159.39 , 154.04 , 145.14 , 145.14 , 145.13 , 132.33 , 126.75 , 123.98 , 123.80 , 115.45 , 111.85 , 72.96 , 21.82 . IR (KBr, cm-1) 3441.1, 3142.3, 2983.3, 1737.5, 1468.7, 1286.3.

*4.1.8.3. Synthesis of 2-[4-isobutoxy-3-(1H-tetrazol-1-yl) phenyl]-6-oxo-1, 6-dihydropyrimidine-5-carboxylic acid (**8c**)*

A white solid, yield: 84.5%. Mp: degraded at 218.3°C. ESI-HRMS calcd. for $C_{16}H_{15}N_6O_4$ $[M - H]^-$ 355.1160, found: 355.1181; ^{1}H NMR (600 MHz, DMSO-d_6) δ 9.82 (s, 1H), 8.73 (s, 1H), 8.56 (d, *J* = 2.2 Hz, 1H), 8.45 (dd, *J* = 8.9, 2.2 Hz, 1H), 7.58 (d, *J* = 9.0 Hz, 1H), 4.02 (d, *J* = 6.4 Hz, 2H), 2.00 (hept, *J* = 6.6 Hz, 1H), 0.88 (d, *J* = 6.7 Hz, 7H) . ^{13}C NMR (100 MHz, DMSO-d_6) δ 165.03 , 159.42 , 155.46 , 145.25 , 145.24 , 145.24 , 132.61 , 126.84 , 124.28 , 123.31 , 114.66 , 111.83 , 75.86 , 27.88 , 19.15 . IR (KBr, cm^{-1}) 3422.9, 3157.8, 2963.6, 1735.4, 1469.3, 1292.3.

*4.1.8.4. Synthesis of 2-[4-(isopentyloxy)-3-(1H-tetrazol-1-yl)phenyl]-6-oxo-1,6-dihydropyrimidine-5-carboxylic acid (**8d**)*

A white solid, yield: 72.6%. Mp: degraded at 210.9°C. ESI-HRMS calcd. for $C_{17}H_{17}N_6O_4$ [M - H]$^-$ 369.1317, found: 369.1383; ^{1}H NMR (600 MHz, DMSO-d_6) δ 9.82 (s, 1H), 8.73 (s, 1H), 8.56 (s, 1H), 8.48 – 8.40 (m, 1H), 7.61 (d, *J* = 8.9 Hz, 1H), 4.26 (t, *J* = 6.1 Hz, 2H), 1.66 – 1.57 (m, 3H), 0.86 (d, *J* = 5.5 Hz, 8H). ^{13}C NMR (100 MHz, DMSO-d_6) δ 164.99 , 159.38 , 155.22 , 145.16 , 145.16 , 145.15 , 132.48 , 126.63 , 124.21 , 123.31 , 114.70 , 111.87 , 68.73 , 37.24 , 25.06 , 22.76 . IR (KBr, cm^{-1}) 3445.8, 3155.8, 2959.3, 1735.5, 1470.3, 1290.7.

*4.1.8.5. Synthesis of 2-[4-(allyloxy)-3-(1H-tetrazol-1-yl) phenyl]-6-oxo-1, 6-dihydropyrimidine-5-carboxylic acid (**8e**)*

A white solid, yield: 80.3%. Mp: degraded at 217.2°C . ESI-HRMS calcd. for $C_{15}H_{11}N_6O_4$ [M - H]$^-$ 339.0847, found: 339.0902; ^{1}H NMR (400 MHz, DMSO-d_6) δ 9.87 (s, 1H), 8.73 (s, 1H), 8.57 (d, *J* = 2.3 Hz, 1H), 8.44 (dd, *J* = 8.8, 2.4 Hz, 1H), 7.58 (d, *J* = 9.0 Hz, 1H), 6.03 (ddt, *J* = 16.1, 10.3, 5.1 Hz, 1H), 5.42 – 5.20 (m, 2H), 4.85 (d, *J* = 5.1 Hz, 2H) . ^{13}C NMR (100 MHz, DMSO-d_6) δ 165.02 , 159.44 , 154.73 , 145.28 , 145.28 , 145.27 , 132.65 , 132.42 , 126.86 , 124.62 , 123.42 , 118.85 , 115.07 , 112.04 , 70.30 . IR (KBr, cm^{-1}) 3188.4, 2927.4, 1750.9, 1442.6, 1282.4.

*4.1.8.6. Synthesis of 2-{4-[(2-methylallyl)oxy]-3-(1H-tetrazol-1-yl)phenyl}-6-oxo-1,6-dihydropyrimidine-5-carboxylic acid (**8f**)*

A white solid, yield: 69.8%. Mp: degraded at 229.6°C. ESI-HRMS calcd. for $C_{16}H_{13}N_6O_4$ [M - H]$^-$ 353.1004, found: 353.1077; ^{1}H NMR (400 MHz, DMSO-d_6) δ 13.44 (s, 2H), 9.84 (s, 1H), 8.73 (s, 1H), 8.55 (s, 1H), 8.44 (d, *J* = 8.9 Hz, 1H), 7.57 (d, *J* = 9.0 Hz, 1H), 4.95 (d, 2H), 4.74 (s, 2H), 1.69 (s, 3H) . ^{13}C NMR (100 MHz, DMSO-d_6) δ 165.01 , 159.41 , 155.06 , 145.36 , 145.35 , 145.34 , 139.88 , 132.56 , 127.14 , 124.57 , 123.40 , 115.04 , 113.52 , 112.01 , 72.82 , 19.40 . IR (KBr, cm^{-1}) 3428.6, 3086.9, 2922.6, 1748.7, 1444.0, 1284.5.

*4.1.8.7. Synthesis of 2-{4-[(3-methylbut-2-en-1-yl) oxy]-3-(1H-tetrazol-1-yl) phenyl}-6-oxo-1, 6-dihydropyrimidine-5-carboxylic acid (**8g**)*

A white solid, yield: 77.8%. Mp>250°C. ESI-HRMS calcd. for $C_{17}H_{15}N_6O_4$ [M - H]$^-$ 367.1160, found: 367.1102; ^{1}H NMR (600 MHz, DMSO-d_6) δ 9.89 (s, 1H), 8.78 (s, 1H), 8.64 (s, 1H), 8.53 (dd, *J* = 8.8, 2.3 Hz, 1H), 7.64 (d, *J* = 8.9 Hz, 1H), 5.49 (t, *J* = 6.8 Hz, 1H), 4.87 (d, *J* = 6.3 Hz, 3H), 1.81 (s, 4H), 1.77 (s, 3H) . ^{13}C NMR (150 MHz, DMSO-d_6) δ 165.89 , 160.52 , 154.52 , 145.15 , 145.15 , 139.35 , 132.12 , 126.42 , 125.86 , 123.34 , 118.90 , 114.97 , 111.26 , 66.88 , 25.89 , 18.59 . IR (KBr, cm^{-1}) 3183.3, 2921.7, 1707.8, 1462.9, 1284.8.

*4.1.8.8. Synthesis of 6-oxo-2-[4-(prop-2-yn-1-yloxy)-3-(1H-tetrazol-1-yl) phenyl]-1, 6-dihydropyrimidine-5-carboxylic acid (**8h**)*

A white solid, yield: 81.7%. Mp: degraded at 223.9°C . ESI-HRMS calcd. for $C_{15}H_9N_6O_4$ [M - H]$^-$ 337.0691, found: 337.0650; ^{1}H NMR (600 MHz, DMSO-d_6) δ 9.87 (s, 1H), 8.74 (s, 1H), 8.59 (d, *J* = 2.0 Hz, 2H), 8.47 (dd, *J* = 8.9, 2.0 Hz, 2H), 7.65 (d, *J* = 9.0 Hz, 1H), 5.10 (d, *J* = 1.8 Hz, 3H), 3.75 (t, *J* = 2.4 Hz, 1H) . ^{13}C NMR (150 MHz, DMSO-d_6) δ 165.07 , 159.42 , 153.67 , 145.27 , 145.25 , 145.24 , 132.25 , 126.92 , 125.37 , 123.58 , 115.29 , 112.08 , 80.33 , 78.23 , 57.79 . IR (KBr, cm^{-1}) 3266.4, 3111.8, 2924.0, 2120.2, 1720.3, 1439.9, 1275.7.

*4.1.8.9. Synthesis of 2-[4-(cyclopropylmethoxy)-3-(1H-tetrazol-1-yl)phenyl]-6-oxo-1,6-dihydropyrimidine-5-carboxylic acid (**8i**)*

A white solid, yield: 74.8%. Mp>250°C. ESI-HRMS calcd. for $C_{16}H_{13}N_6O_4$ [M - H]$^-$ 353.1004, found: 353.1038; ^{1}H NMR (600 MHz, DMSO-d_6) δ 13.67 (s, 1H), 9.84 (s, 1H), 8.71 (s, 1H), 8.58 (s, 1H), 8.40 (d, *J* = 7.5 Hz, 1H), 7.55 (d, *J* = 8.2 Hz, 1H), 4.12 (d, *J* = 5.6 Hz, 2H), 1.30 – 1.17 (m, 1H), 0.55 (d, *J* = 7.9 Hz, 2H), 0.38 – 0.29 (m, 2H) . ^{13}C NMR (100 MHz, DMSO-d_6) δ 164.94 , 159.29 , 154.91 , 145.02 , 145.02 , 145.01 , 132.25 , 126.26 , 124.14 , 123.36 , 114.89 , 111.79 , 74.59 , 10.01 , 3.44 . IR (KBr, cm^{-1}) 3187.6, 2925.5, 1698.9, 1468.3, 1288.4.

*4.1.8.10. Synthesis of 2-[4-(cyclopentyloxy)-3-(1H-tetrazol-1-yl) phenyl]-6-oxo-1, 6-dihydropyrimidine-5-carboxylic acid (**8J**)*

A white solid, yield: 76.3%. Mp>250°C. ESI-HRMS calcd. for $C_{17}H_{15}N_6O_4$ [M - H]$^-$ 367.1160, found: 367.1173; ^{1}H NMR (600 MHz, DMSO-d_6) δ 9.78 (s, 1H), 8.71 (s, 1H), 8.56 (s, 1H), 8.43 (d, *J* = 8.8 Hz, 1H), 7.57 (d, *J* = 8.9 Hz, 1H), 5.13 (t, *J* = 6.0 Hz, 1H), 1.93 (dt, *J* = 13.5, 6.7 Hz, 2H), 1.79 – 1.67 (m, 2H), 1.63 – 1.50 (m, 5H) . ^{13}C NMR (100 MHz, DMSO-d_6) δ 165.15 , 159.59 , 154.16 , 145.09 , 145.08 , 145.08 , 132.29 , 126.73 , 124.30 , 123.86 , 115.58 , 111.71 , 82.07 , 32.54 , 23.82 . IR (KBr, cm^{-1}) 3446.9, 2958.8, 1736.8, 1430.3, 1285.1.

*4.1.8.11. Synthesis of 2-[4-(cyclohexylmethoxy)-3-(1H-tetrazol-1-yl)phenyl]-6-oxo-1,6-dihydropyrimidine-5-carboxylic acid (**8k**)*

A white solid, yield: 78.2%. Mp: degraded at 211.0°C. ESI-HRMS calcd. for $C_{19}H_{19}N_6O_4$ [M - H]$^-$ 395.1473,

found: 395.1485; ^{1}H NMR (600 MHz, DMSO-d_6) δ 9.81 (s, 1H), 8.73 (s, 1H), 8.55 (d, *J* = 2.1 Hz, 1H), 8.44 (dd, *J* = 8.9, 2.1 Hz, 1H), 7.59 (d, *J* = 9.0 Hz, 1H), 4.04 (d, *J* = 6.3 Hz, 2H), 1.77 – 1.58 (m, 6H), 1.24 – 1.17 (m, 2H), 1.14 – 1.06 (m, 1H), 1.01 – 0.90 (m, 2H) . ^{13}C NMR (100 MHz, DMSO-d_6) δ 165.03 , 159.43 , 155.48 , 145.24 , 145.23 , 145.23 , 132.59 , 126.82 , 124.25 , 123.31 , 114.67 , 111.85 , 74.93 , 37.08 , 29.31 , 26.36 , 25.57 . IR (KBr, cm^{-1}) 3189.1, 2930.1, 1707.2, 1465.8, 1287.9.

*4.1.8.12. Synthesis of 2-[4-(benzyloxy)-3-(1H-tetrazol-1-yl)phenyl]-6-oxo-1,6-dihydropyrimidine-5-carboxylic acid (**8l**)*

A white solid, yield: 80.8%. Mp: degraded at 214.6°C. ESI-HRMS calcd. for $C_{19}H_{13}N_6O_4$ [M - H]$^-$ 389.1004, found: 389.0974; ^{1}H NMR (600 MHz, DMSO-d_6) δ 9.86 (s, 1H), 8.72 (s, 1H), 8.58 (d, *J* = 2.3 Hz, 1H), 8.44 (dd, *J* = 8.9, 2.4 Hz, 1H), 7.67 (d, *J* = 8.9 Hz, 1H), 7.45 – 7.30 (m, 6H), 5.38 (s, 2H). ^{13}C NMR (100 MHz, DMSO-d_6) δ 165.73 , 160.36 , 154.56 , 145.24 , 145.24 , 145.23 , 136.01 , 132.30 , 129.03 , 128.73 , 128.06 , 126.75 , 126.05 , 123.45 , 115.10 , 111.52 , 71.32 . IR (KBr, cm^{-1}) 3417.2, 2944.3, 1717.7, 1454.4, 1285.1.

*4.1.8.13. Synthesis of 2-{4-[(4-methylbenzyl) oxy]-3-(1H-tetrazol-1-yl) phenyl}-6-oxo-1, 6-dihydropyrimidine-5-carboxylic acid (**8m**)*

A white solid, yield: 84.1%. Mp>250°C. ESI-HRMS calcd. for $C_{20}H_{15}N_6O_4$ [M - H]$^-$ 403.1160, found: 403.1245; ^{1}H NMR (600 MHz, DMSO-d_6) δ 9.81 (s, 1H), 8.64 (s, 1H), 8.55 (s, 1H), 8.51 (d, *J* = 8.7 Hz, 1H), 7.50 (s, 1H), 7.28 (d, *J* = 6.5 Hz, 3H), 7.18 (d, *J* = 7.3 Hz, 3H), 5.24 (s, 2H), 2.29 (s, 3H) . ^{13}C NMR (150 MHz, DMSO-d_6) δ 162.58 , 159.49 , 152.24 , 145.18 , 145.17 , 145.16 , 137.89 , 133.37 , 131.32 , 129.51 , 128.15 , 125.64 , 123.10 , 122.79 , 116.38 , 114.11 , 70.81 , 21.23 . IR (KBr, cm^{-1}) 3421.9, 2924.0, 1599.7, 1437.9, 1286.3.

*4.1.8.14. Synthesis of 2-{4-{[4-(tert-butyl) benzyl] oxy}-3-(1H-tetrazol-1-yl) phenyl}-6-oxo-1, 6-dihydropyrimidine-5-carboxylic acid (**8n**)*

A white solid, yield: 76.6%. Mp: degraded at 155.9°C. ESI-HRMS calcd. for $C_{23}H_{21}N_6O_4$ [M - H]$^-$ 445.1630, found: 445.1683; ^{1}H NMR (600 MHz, DMSO-d_6) δ 9.84 (s, 1H), 8.64 (s, 1H), 8.56 (d, *J* = 2.2 Hz, 1H), 8.52 (dd, *J* = 8.8, 2.2 Hz, 1H), 7.56 (d, *J* = 8.9 Hz, 1H), 7.40 (d, *J* = 8.4 Hz, 2H), 7.33 (d, *J* = 8.2 Hz, 2H), 5.28 (s, 2H), 1.27 (s, 9H) . ^{13}C NMR (100 MHz, DMSO-d_6) δ 165.13 , 159.55 , 154.90 , 151.26 , 145.23 , 145.23 , 145.23 , 132.91 , 132.45 , 127.94 , 126.85 , 125.78 , 124.84 , 123.48 , 115.15 , 111.88 , 71.21 , 34.79 , 31.53 . IR (KBr,

cm^{-1}) 3423.5, 2961.4, 1737.7, 1463.2, 1273.0.

*4.1.8.15. Synthesis of 2-{4-[(4-methoxybenzyl)oxy]-3-(1H-tetrazol-1-yl)phenyl}-6-oxo-1,6-dihydropyrimidine-5-carboxylic acid (**8o**)*

A white solid, yield: 70.1%. Mp: degraded at 118.8°C. ESI-HRMS calcd. for $C_{20}H_{15}N_6O_5$ $[M - H]^-$ 419.1109, found: 419.1009; ^{1}H NMR (600 MHz, DMSO-d_6) δ 14.00 (s, 1H), 9.81 (s, 1H), 8.72 (s, 1H), 8.57 (d, *J* = 2.3 Hz, 1H), 8.45 (dd, *J* = 8.9, 2.3 Hz, 1H), 7.68 (d, *J* = 9.0 Hz, 1H), 7.37 (d, *J* = 8.5 Hz, 2H), 6.94 (d, *J* = 8.6 Hz, 2H), 5.29 (s, 2H), 3.75 (s, 3H) . ^{13}C NMR (150 MHz, DMSO-d_6) δ 165.46 , 159.97 , 159.77 , 154.69 , 145.18 , 145.17 , 145.15 , 132.29 , 130.11 , 127.73 , 126.67 , 125.34 , 123.46 , 115.18 , 114.41 , 111.67 , 71.24 , 55.57 . IR (KBr, cm^{-1}) 3409.1, 3160.0, 2933.0, 1722.0, 1482.2, 1297.8.

*4.1.8.16. Synthesis of 2-{4-[(4-fluorobenzyl)oxy]-3-(1H-tetrazol-1-yl)phenyl}-6-oxo-1,6-dihydropyrimidine-5-carboxylic acid (**8p**)*

A white solid, yield: 76.5%. Mp: degraded at 213.9°C. ESI-HRMS calcd. for $C_{19}H_{12}FN_6O_4$ $[M - H]^-$ 407.0910, found: 407.0808; ^{1}H NMR (600 MHz, DMSO-d_6) δ 9.85 (s, 1H), 8.73 (s, 1H), 8.58 (s, 1H), 8.45 (d, *J* = 8.9 Hz, 1H), 7.67 (d, *J* = 8.8 Hz, 1H), 7.53 – 7.43 (m, 2H), 7.29 – 7.17 (m, 2H), 5.36 (s, 2H) . ^{13}C NMR (100 MHz, DMSO-d_6) δ 165.05 , 159.45 , 154.70 , 145.18 , 132.42 , 132.15 , 130.56 , 130.47 , 126.84 , 124.85 , 123.51 , 116.01 , 115.79 , 115.17 , 70.69 . IR (KBr, cm^{-1}) 3419.5, 3173.6, 3078.6, 1723.0, 1462.3, 1286.4.

*4.1.8.17. Synthesis of 2-{4-[(4-chlorobenzyl) oxy]-3-(1H-tetrazol-1-yl) phenyl}-6-oxo-1, 6-dihydropyrimidine-5-carboxylic acid (**8q**)*

A white solid, yield: 78.2%. Mp>250°C. ESI-HRMS calcd. for $C_{19}H_{12}ClN_6O_4$ $[M - H]^-$ 423.0614, found: 423.0579; ^{1}H NMR (400 MHz, DMSO-d_6) δ 13.94 (s, 1H), 9.86 (s, 1H), 8.72 (s, 1H), 8.58 (d, *J* = 2.3 Hz, 1H), 8.45 (dd, *J* = 8.9, 2.4 Hz, 1H), 7.65 (d, *J* = 9.0 Hz, 1H), 7.50 – 7.41 (m, 4H), 5.38 (s, 2H). ^{13}C NMR (100 MHz, DMSO-d_6) δ 165.35 , 159.83 , 154.53 , 145.23 , 145.22 , 145.22 , 135.00 , 133.42 , 132.38 , 130.03 , 129.06 , 126.84 , 125.46 , 123.49 , 115.14 , 111.78 , 70.54 . IR (KBr, $cm^{-1)}$ 3440.1, 3089.8, 2923.3, 1723.2, 1461.4, 1288.2.

*4.1.8.18. Synthesis of 2-{4-[(4-bromobenzyl)oxy]-3-(1H-tetrazol-1-yl)phenyl}-6-oxo-1,6-dihydropyrimidine-5-carboxylic acid (**8r**)*

A white solid, yield: 80.6%. Mp>250°C. ESI-HRMS calcd. for $C_{19}H_{12}BrN_6O_4$ [M - H]$^-$ 467.0109, found: 466.9961; ^{1}H NMR (600 MHz, DMSO-d_6) δ 14.24 (s, 1H), 9.87 (s, 1H), 8.72 (s, 1H), 8.58 (s, 1H), 8.46 (d, *J* = 8.9 Hz, 1H), 7.63 (d, *J* = 8.8 Hz, 1H), 7.60 (d, *J* = 7.6 Hz, 2H), 7.38 (d, *J* = 7.3 Hz, 2H), 5.36 (s, 2H) . ^{13}C NMR (150 MHz, DMSO-d_6) δ 165.79 , 160.40 , 154.31 , 145.26 , 145.24 , 135.46 , 132.27 , 131.99 , 130.34 , 126.75 , 126.25 , 123.43 , 121.98 , 115.06 , 111.53 , 70.51 , 40.51 . IR (KBr, cm^{-1}) 3420.2, 2925.9, 1734.8, 1490.4, 1289.5.

*4.1.8.19. Synthesis of 2-{4-[(3-methoxybenzyl) oxy]-3-(1H-tetrazol-1-yl) phenyl}-6-oxo-1, 6-dihydropyrimidine-5-carboxylic acid (**8s**)*

A white solid, yield: 68.6%. Mp: degraded at 228.3°C. ESI-HRMS calcd. for $C_{20}H_{15}N_6O_5$ [M - H]$^-$ 419.1109, found: 419.1086; ^{1}H NMR (600 MHz, DMSO-d_6) δ 13.82 (s, 1H), 9.90 (s, 1H), 8.73 (s, 1H), 8.58 (s, 1H), 8.45 (d, *J* = 8.9 Hz, 1H), 7.66 (d, *J* = 9.0 Hz, 1H), 7.30 (t, *J* = 7.9 Hz, 1H), 6.97 (s, 2H), 6.90 (d, *J* = 8.1 Hz, 1H), 5.35 (s, 2H), 3.74 (s, 3H). ^{13}C NMR (100 MHz, DMSO-d_6) δ 165.09 , 159.83 , 159.50 , 154.84 , 145.28 , 145.28 , 145.27 , 137.49 , 132.48 , 130.14 , 126.89 , 124.86 , 123.53 , 119.97 , 115.16 , 114.29 , 113.30 , 111.94 , 71.18 , 55.50 . IR (KBr, cm^{-1}) 3444.6, 3094.4, 1743.1, 1448.2, 1290.7.

*4.1.8.20. Synthesis of 2-{4-[(3-fluorobenzyl) oxy]-3-(1H-tetrazol-1-yl)phenyl}-6-oxo-1,6-dihydropyrimidine-5-carboxylic acid (**8t**)*

A white solid, yield: 83.9%. Mp: degraded at 212.7°C. ESI-HRMS calcd. for $C_{19}H_{12}FN_6O_4$ [M - H]$^-$ 407.0910, found: 407.0945; ^{1}H NMR (600 MHz, DMSO-d_6) δ 9.90 (s, 1H), 8.72 (s, 1H), 8.58 (d, *J* = 2.3 Hz, 1H), 8.44 (dd, *J* = 8.8, 2.4 Hz, 1H), 7.64 (d, *J* = 8.9 Hz, 1H), 7.44 (q, *J* = 7.5 Hz, 1H), 7.29 – 7.22 (m, 2H), 7.18 (t, *J* = 7.5 Hz, 1H), 5.40 (s, 2H). ^{13}C NMR (100 MHz, DMSO-d_6) δ 163.84 , 161.41 , 154.43 , 145.29 , 138.89 , 138.82 , 132.38 , 131.15 , 131.07 , 126.85 , 123.96 , 123.48 , 115.63 , 115.43 , 115.06 , 114.85 , 114.63 , 111.69 , 70.46 . IR (KBr, cm^{-1}) 3454.2, 3076.1, 2923.4, 1749.6, 1457.3, 1285.6.

*4.1.8.21. Synthesis of 2-{4-[(3-chlorobenzyl)oxy]-3-(1H-tetrazol-1-yl)phenyl}-6-oxo-1,6-dihydropyrimidine-5-carboxylic acid (**8u**)*

A white solid, yield: 81.7%. Mp>250°C. ESI-HRMS calcd. for $C_{19}H_{12}ClN_6O_4$ [M - H]$^-$ 423.0614, found: 423.0588; ^{1}H NMR (600 MHz, DMSO-d_6) δ 13.77 (s, 1H), 9.90 (s, 1H), 8.72 (s, 1H), 8.58 (s, 1H), 8.44 (d, *J* = 8.8 Hz, 1H), 7.64 (d, *J* = 7.0 Hz, 1H), 7.49 (s, 1H), 7.45 – 7.39 (m, 2H), 7.37 (d, *J* = 6.7 Hz, 1H), 5.39 (s, 2H) .

^{13}C NMR (150 MHz, DMSO-d_6) δ 165.14 , 159.50 , 154.54 , 145.28 , 145.26 , 145.25 , 138.45 , 133.68 , 132.45 , 130.96 , 128.68 , 127.83 , 126.87 , 126.59 , 125.08 , 123.49 , 115.09 , 111.92 , 70.41 . IR (KBr, cm^{-1}) 3460.3, 3074.6, 2927.5, 1714.0, 1462.3, 1273.9.

*4.1.8.22. Synthesis of 2-{4-[(3-bromobenzyl) oxy]-3-(1H-tetrazol-1-yl) phenyl}-6-oxo-1, 6-dihydropyrimidine-5-carboxylic acid (**8v**)*

A white solid, yield: 74.4%. Mp>250°C. ESI-HRMS calcd. for $C_{19}H_{12}BrN_6O_4$ $[M - H]^-$ 467.0109, found: 467.0154; ^{1}H NMR (600 MHz, DMSO-d_6) δ 13.69 (s, 1H), 9.90 (s, 1H), 8.73 (s, 1H), 8.58 (s, 1H), 8.44 (dd, *J* = 8.9, 2.4 Hz, 1H), 7.64 (d, *J* = 9.8 Hz, 2H), 7.54 (d, *J* = 7.7 Hz, 1H), 7.43 – 7.39 (m, 1H), 7.36 (t, *J* = 7.8 Hz, 1H), 5.39 (s, 2H) . ^{13}C NMR (100 MHz, DMSO-d_6) δ 165.04 , 159.42 , 154.60 , 145.25 , 145.24 , 145.24 , 138.69 , 132.47 , 131.58 , 131.22 , 130.72 , 126.97 , 126.90 , 124.96 , 123.53 , 122.24 , 115.12 , 111.98 , 70.38 . IR (KBr, cm^{-1}) 3180.6, 2931.6, 1701.7, 1470.7, 1272.4.

*4.1.8.23. Synthesis of 2-{4-[(2-chlorobenzyl) oxy]-3-(1H-tetrazol-1-yl) phenyl}-6-oxo-1, 6-dihydropyrimidine-5-carboxylic acid (**8w**)*

A white solid, yield: 76.8%. Mp: degraded at 196.1°C. ESI-HRMS calcd. for $C_{19}H_{12}ClN_6O_4$ $[M - H]^-$ 423.0614, found: 423.0661; ^{1}H NMR (400 MHz, DMSO-d_6) δ 9.78 (s, 1H), 8.74 (s, 1H), 8.59 (d, *J* = 2.4 Hz, 1H), 8.48 (dd, *J* = 8.9, 2.3 Hz, 1H), 7.74 (d, *J* = 9.0 Hz, 1H), 7.55 – 7.47 (m, 2H), 7.45 – 7.33 (m, 2H), 5.45 (s, 2H) . ^{13}C NMR (100 MHz, DMSO-d_6) δ 165.04 , 159.43 , 154.66 , 145.21 , 145.21 , 145.20 , 133.26 , 133.04 , 132.59 , 130.83 , 130.52 , 130.03 , 127.92 , 127.04 , 125.12 , 123.57 , 115.28 , 112.06 , 69.12 . IR (KBr, cm^{-1}) 3402.8, 3167.9, 2924.9, 1711.8, 1476.6, 1295.0.

*4.1.8.24. Synthesis of 2-{4-[(2, 6-dichlorobenzyl) oxy]-3-(1H-tetrazol-1-yl) phenyl}-6-oxo-1, 6-dihydropyrimidine-5-carboxylic acid (**8x**)*

A white solid, yield: 71.5%. Mp: degraded at 171.4°C. ESI-HRMS calcd. for $C_{19}H_{12}Cl_2N_6O_4$ $[M - H]^-$ 457.0224, found: 457.0284; ^{1}H NMR (400 MHz, DMSO-d_6) δ 9.57 (s, 1H), 8.74 (s, 1H), 8.57 (d, *J* = 2.3 Hz, 1H), 8.52 (dd, *J* = 8.9, 2.4 Hz, 1H), 7.89 (d, *J* = 8.9 Hz, 1H), 7.60 – 7.51 (m, 2H), 7.46 (dd, *J* = 9.1, 6.9 Hz, 1H), 5.52 (s, 2H) . ^{13}C NMR (100 MHz, DMSO-d_6) δ 165.01 , 159.36 , 154.83 , 145.00 , 145.00 , 144.99 , 136.40 , 132.68 , 132.55 , 130.62 , 129.36 , 127.10 , 125.44 , 123.65 , 115.49 , 112.12 , 67.36 . IR (KBr, cm^{-1}) 3405.1, 3066.1, 2922.6, 1720.8, 1479.1, 1291.1.

*4.1.8.25. Synthesis of 2-{4-[(2,4-dichlorobenzyl)oxy]-3-(1H-tetrazol-1-yl)phenyl}-6-oxo-1,6-dihydropyrimidine-5-carboxylic acid (**8y**)*

A white solid, yield: 75.8%. Mp: degraded at 224.4°C. ESI-HRMS calcd. for $C_{19}H_{12}Cl_2N_6O_4$ [M - H]$^-$ 457.0224, found: 457.0231; ^{1}H NMR (400 MHz, DMSO-d_6) δ 9.78 (s, 1H), 8.74 (s, 1H), 8.58 (d, *J* = 2.3 Hz, 1H), 8.47 (dd, *J* = 8.8, 2.3 Hz, 1H), 7.73 (d, *J* = 9.0 Hz, 1H), 7.70 (d, *J* = 1.9 Hz, 1H), 7.55 – 7.45 (m, 2H), 5.43 (s, 2H) . ^{13}C NMR (100 MHz, DMSO-d_6) δ 165.06 , 159.46 , 154.66 , 145.21 , 145.21 , 145.21 , 133.26 , 133.04 , 132.59 , 130.83 , 130.53 , 130.03 , 127.92 , 127.04 , 125.16 , 123.57 , 115.28 , 112.03 , 69.12 . IR (KBr, cm^{-1}) 3149.8, 3086.9, 1718.1, 1461.3, 1283.9.

*4.1.9. Synthesis of 2-[4-hydroxy-3-(1H-tetrazol-1-yl)phenyl]-6-oxo-1,6-dihydropyrimidine-5-carboxylic acid (**8z**)*

A mixture of compound **8l** (500 mg, 1.28 mmol) and 10% Pd/C (50 mg) in DMF was stirred at room temperature for 6 h under hydrogen atmosphere. After the completion of the reaction, the Pd/C was filtered out and the filtrate was evaporated to obtain 2-[4-hydroxy-3-(1*H*-tetrazol-1-yl) phenyl]-6-oxo-1, 6-dihydropyrimidine-5-carboxylic acid **8z**, a brown solid (281 mg, 73.1%), mp>250°C. ESI-HRMS calcd. for $C_{12}H_7N_6O_4$ [M - H]$^-$ 299.0534, found: 299.0576; ^{1}H NMR (600 MHz, DMSO-d_6) δ 13.80 (s, 1H), 12.14 (s, 1H), 9.87 (s, 1H), 8.69 (s, 1H), 8.56 (s, 1H), 8.30 (d, *J* = 8.8 Hz, 1H), 7.32 (d, *J* = 8.8 Hz, 1H) . ^{13}C NMR (150 MHz, DMSO-d_6) δ 165.16 , 159.67 , 154.94 , 145.02 , 145.00 , 144.98 , 132.09 , 126.62 , 123.02 , 122.21 , 117.89 , 111.36. IR (KBr, cm^{-1}) 3561.9, 3126.7, 1727.2, 1480.2, 1316.6.

4.2. Assay for the in vitro XOR inhibitory activity

The XO inhibitory potency with xanthine as the substrate was assayed spectrophotometrically by measuring uric acid formation at 295 nm at 25°C according to the procedure reported by Matsumoto *et al*. [12] with modification. XO (Sigma, X4875) was suspended in a buffer (0.1 M sodium pyrophosphate and 0.3 mM Na_2EDTA buffer, pH 8.3). Xanthine (J&K) was dissolved and diluted with the buffer to obtain the substrate solution (500 μM). The tested compounds were initially dissolved in DMSO to yield a 10000 μM solution, which was then further diluted with buffer to obtain the required concentrations. The buffer (67 μL), enzyme solution (75 U/L, 40 μL) and sample (53 μL) or blank solution (the buffer) were added to 96-well plates

(COSTAR 3599) and incubated at 25 °C for 15 min. Then, the mixture was added with substrate (40 μL) to the plates to a total volume of 200 μL, which was further scanned to measure the absorbance change immediately at 295 nm and at 30 s intervals for 2 min. Febuxostat and allopurinol were used as positive controls. All the tests were performed in triplicate. Compounds presenting inhibitory effects over 50% at a concentration of 10 μM were further tested at a wide range of concentrations to calculate their IC_{50} values using SPSS 20.0 software (SPSS Inc, Chicago, IL, USA). Enzyme kinetic assays were performed in the same way as the XO assay but with varying concentrations of the substrate at 400, 500, 600 and 700 μM (final concentrations of the substrate were 80, 100, 120 and 140 μM, respectively).

4.3. Molecular modeling

Molecular docking studies were performed using GLIDE (2016, Schrodinger Suite) [60]. The crystal structure of xanthine dehydrogenase (XDH) with febuxostat (1N5X.pdb) was retrieved from the RCSB Protein Data Bank. All bound water was eliminated from the protein, and all hydrogen atoms were added to the proteins. The protein was prepared, optimized and minimized by Protein Preparation Wizard using an OPLS-2005 force field (2016, Schrodinger Suite). The ligands were built within Maestro BUILD (2016, Schrodinger Suite) and prepared by the LIGPREP module (2016, Schrodinger Suite). The tautomeric forms of ligands, which include the keto and enol forms of ligands, were generated at a physiological pH (7.0 ± 2.0 pH) [61]. The active site for docking was defined as a grid box of dimensions 25×25×25 $Å^3$ [61] around the centroid of the ligand, assuming that the ligands to be docked were of a size similar to the cocrystallized ligand. The docking methodology has been validated by extracting the crystallographic bound febuxostat and redocking it with the Glide module using extra precision (XP) to the catalytic site of 1N5X. This validation provided a root mean square deviation (rmsd) of 0.046 Å between the docked versus the experimental conformation [61]. Different docking poses of ligands were generated and analyzed for interpretation of the final results. Accelrys Discovery Studio Visualizer 2017 [62] and Pymol [63] were used for graphic display.

4.4. Steady-state kinetic analysis

The representative compound **8u** was further investigated for the type of inhibition and an enzyme kinetics

study was carried out. The Lineweaver–Burk plot was established from which we could calculate the K_m, V_{max} of the slope of the inhibitor and the value of α (a constant that defines the degree to which inhibitor binding affects the affinity of the enzyme for the substrate).

4.5. Acute oral toxicity study

Healthy Kunming mice of both sexes (18–22 g; Number of Approval of Ethics Committee: SYPU-IACUC-2019-6-26-106) were purchased from the Animal Center of Shenyang Pharmaceutical University (Shenyang, China). Animal maintenance and treatment met the protocols approved by the Ethics Review Committee for Animal Experimentation of Shenyang Pharmaceutical University. The mice had free access to food and water and were maintained on a 12-h light/dark cycle in a temperature- and humidity-controlled room for one week.

After fasting for 12 h with free access to water prior to the experiment, two groups of animals each consisting of 6 mice were employed for acute oral toxicity study for the compound **8u**. The first group was treated with the 0.5% CMC-Na and served as the vehicle control. The remaining group was treated with a single higher dose (2000 mg/kg) of the test compound **8u**, which was dissolved in 0.5% CMC-Na solution. All the treatments were intragastrically administered immediately after 12 h of fasting. The animals were observed continuously for any signs and symptoms of toxicity for 24 h after treatment.

4.6. In vivo hypouricemic effect assay

Male Sprague-Dawley rats (6 weeks old, n=8; Number of Approval of Ethics Committee: SYPU-IACUC-2019-1-11-203) were purchased from the Animal Center of Shenyang Pharmaceutical University (Shenyang, China). Animal maintenance and treatment met the protocols approved by the Ethics Review Committee for Animal Experimentation of Shenyang Pharmaceutical University. The rats had free access to food and water and were maintained on a 12-h light/dark cycle in a temperature- and humidity-controlled room for one week.

After fasting for 12 h with free access to water prior to the experiment, rats were randomly divided into five groups and intragastrically administered febuxostat (5 mg/kg), allopurinol (10 mg/kg) and the test compound **8u** (5 mg/kg), which was dissolved in 0.5% CMC-Na solution [19], whereas the other two groups were treated with

0.5% CMC-Na. Febuxostat and allopurinol were used as the positive control drugs. Then, rats except those in the blank group were injected intraperitoneally with potassium oxonate (300 mg/kg) 1 h after drug administration to increase the serum urate levels [64-66]. Blood samples were collected from the rats via orbital vein bleeding at 2, 3, 4, 6 and 8 h after drug administration. The collected blood samples were allowed to clot at room temperature for 2 h, followed by centrifuging at 3000 g at 4°C for 10 min. Serum urate levels were determined with a uric acid assay kit (Nanjing Jiancheng Bioengineering Institute, China) in accordance with the manufacturer's instructions.

The statistical analysis was performed using Student's *t*-test to determine the level of significance. Data are presented as the means ± S.Ds. The figures were obtained with the GraphPad 6.0 statistical system.

Acknowledgments

This work was supported by the National Natural Science Foundation of China (Grant No.81773813). Specifically, we are grateful to Professor Zheng Liu and his team for their support in the *in vivo* hypouricemic effect assay.

References

[1] G. Luna, A.V. Dolzhenko, R.L. Mancera, Inhibitors of xanthine oxidase: scaffold diversity and structure-based drug design, ChemMedChem, 14 (2019) 714-743.

[2] M. Gliozzi, N. Malara, S. Muscoli, V. Mollace, The treatment of hyperuricemia, International journal of cardiology, 213 (2016) 23-27.

[3] R. Ojha, J. Singh, A. Ojha, H. Singh, S. Sharma, K. Nepali, An updated patent review: xanthine oxidase inhibitors for the treatment of hyperuricemia and gout (2011-2015), Expert opinion on therapeutic patents, 27 (2017) 311-345.

[4] C. Chen, J.-M. Lü, Q. Yao, Hyperuricemia-related diseases and xanthine oxidoreductase (XOR) inhibitors: an overview, Medical science monitor, 22 (2016) 2501-2512.

[5] R. Kaur, F. Naaz, S. Sharma, S. Mehndiratta, M.K. Gupta, P.M.S. Bedi, K. Nepali, Screening of a library of 4-aryl/heteroaryl-4H-fused pyrans for xanthine oxidase inhibition: synthesis, biological evaluation and docking studies, Medicinal Chemistry Research, 24 (2015) 3334-3349.

[6] H.S. Virdi, S. Sharma, S. Mehndiratta, P.M. Bedi, K. Nepali, Design, synthesis and evaluation of 2,4-diarylpyrano[3,2-c]chromen-5(4H)-one as a new class of non-purine xanthine oxidase inhibitors, Journal of enzyme inhibition and medicinal chemistry, (2014) 1-7.

[7] M. Leigh, D.J. Raines, C.E. Castillo, A.K. Duhme-Klair, Inhibition of xanthine oxidase by thiosemicarbazones, hydrazones and dithiocarbazates derived from hydroxy-substituted benzaldehydes, ChemMedChem, 6 (2011) 1107-1118.

[8] J.V. Singh, G. Mal, G. Kaur, M.K. Gupta, A. Singh, K. Nepali, H. Singh, S. Sharma, S.B. PM, Benzoflavone derivatives as potent antihyperuricemic agents, MedChemComm, 10 (2019) 128-147.

[9] R. Kumar, Darpan, S. Sharma, R. Singh, Xanthine oxidase inhibitors: a patent survey, Expert opinion on therapeutic patents, 21 (2011) 1071-1108.

[10] R. Dhiman, S. Sharma, G. Singh, K. Nepali, P.M. Singh Bedi, Design and synthesis of aza-flavones as a new class of xanthine oxidase inhibitors, Arch Pharm (Weinheim), 346 (2013) 7-16.

[11] K. Okamoto, B.T. Eger, T. Nishino, S. Kondo, E.F. Pai, T. Nishino, An extremely potent inhibitor of xanthine oxidoreductase. Crystal structure of the enzyme-inhibitor complex and mechanism of inhibition, The Journal of biological chemistry, 278 (2003) 1848-1855.

[12] K. Matsumoto, K. Okamoto, N. Ashizawa, T. Nishino, FYX-051: A Novel and Potent Hybrid-Type Inhibitor of Xanthine Oxidoreductase, Journal of Pharmacology and Experimental Therapeutics, 336 (2010) 95-103.

[13] S. Ishibuchi, H. Morimoto, T. Oe, T. Ikebe, H. Inoue, A. Fukunari, M. Kamezawa, I. Yamada, Y. Naka, Synthesis and structure–activity relationships of 1-phenylpyrazoles as xanthine oxidase inhibitors, Bioorganic &

medicinal chemistry letters, 11 (2001) 879-882.

[14] S. Wang, J. Yan, J. Wang, J. Chen, T. Zhang, Y. Zhao, M. Xue, Synthesis of some 5-phenylisoxazole-3-carboxylic acid derivatives as potent xanthine oxidase inhibitors, European journal of medicinal chemistry, 45 (2010) 2663-2670.

[15] Q. Guan, Z. Cheng, X. Ma, L. Wang, D. Feng, Y. Cui, K. Bao, L. Wu, W. Zhang, Synthesis and bioevaluation of 2-phenyl-4-methyl-1,3-selenazole-5-carboxylic acids as potent xanthine oxidase inhibitors, European journal of medicinal chemistry, 85 (2014) 508-516.

[16] S. Chen, T. Zhang, J. Wang, F. Wang, H. Niu, C. Wu, S. Wang, Synthesis and evaluation of 1-hydroxy/methoxy-4-methyl-2-phenyl-1*H*-imidazole-5-carboxylic acid derivatives as non-purine xanthine oxidase inhibitors, European journal of medicinal chemistry, 103 (2015) 343-353.

[17] J.U. Song, S.P. Choi, T.H. Kim, C.K. Jung, J.Y. Lee, S.H. Jung, G.T. Kim, Design and synthesis of novel 2-(indol-5-yl)thiazole derivatives as xanthine oxidase inhibitors, Bioorganic & medicinal chemistry letters, 25 (2015) 1254-1258.

[16-18] T.J. Zhang, Q.X. Wu, S.Y. Li, L. Wang, Q. Sun, Y. Zhang, F.H. Meng, H. Gao, Synthesis and evaluation of 1-phenyl-1*H*-1,2,3-triazole-4-carboxylic acid derivatives as xanthine oxidase inhibitors, Bioorganic & medicinal chemistry letters, 27 (2017) 3812-3816.

[19] J. Li, F. Wu, X. Liu, Y. Zou, H. Chen, Z. Li, L. Zhang, Synthesis and bioevaluation of 1-phenyl-pyrazole-4-carboxylic acid derivatives as potent xanthine oxidoreductase inhibitors, European journal of medicinal chemistry, 140 (2017) 20-30.

[20] M. Kawakami, Y. Keto, K. Ikeda, M. Fukuda, J. Sato, Treatment of a stomach or small intestine ulcer with 2-(3-cyano-4-isobutyloxyphenyl)-4-methyl-1, 3-thiazole-5-carboxylic acid, U.S. Patent 8,426,453[P]. 2013-4-23.

[21] A. Shi, L. Zhang, H. Wang, S. Wang, M. Yang, Q. Guan, K. Bao, W. Zhang, Design, synthesis and bioevaluation of 2-mercapto-6-phenylpyrimidine-4-carboxylic acid derivatives as potent xanthine oxidase inhibitors, European journal of medicinal chemistry, 155 (2018) 590-595.

[22] S. Khanna, S. Burudkar, K. Bajaj, P. Shah, A. Keche, U. Ghosh, A. Desai, A. Srivastava, A. Kulkarni-Almeida, N.J. Deshmukh, A. Dixit, M.K. Brahma, U. Bahirat, L. Doshi, K.V. Nemmani, P. Tannu, A. Damre, B.R. C, R. Sharma, H. Sivaramakrishnan, Isocytosine-based inhibitors of xanthine oxidase: design, synthesis, SAR, PK and in vivo efficacy in rat model of hyperuricemia, Bioorganic & medicinal chemistry letters, 22 (2012) 7543-7546.

[23] J. Evenas, F. Edfeldt, M. Lepisto, N. Svitacheva, A. Synnergren, B. Lundquist, M. Granse, A. Ronnholm, M. Varga, J. Wright, M. Wei, S. Yue, J. Wang, C. Li, X. Li, G. Chen, Y. Liao, G. Lv, A. Tjornebo, F. Narjes, HTS followed by NMR based counterscreening. Discovery and optimization of pyrimidones as reversible and competitive

inhibitors of xanthine oxidase, Bioorganic & medicinal chemistry letters, 24 (2014) 1315-1321.

[24] M. Kaur, A. Kaur, S. Mankotia, H. Singh, A. Singh, J.V. Singh, M.K. Gupta, S. Sharma, K. Nepali, P.M.S. Bedi, Synthesis, screening and docking of fused pyrano[3,2-d]pyrimidine derivatives as xanthine oxidase inhibitor, European journal of medicinal chemistry, 131 (2017) 14-28.

[25] L. Zhang, S. Wang, M. Yang, A. Shi, H. Wang, Q. Guan, K. Bao, W. Zhang, Design, synthesis and bioevaluation of 3-oxo-6-aryl-2,3-dihydropyridazine-4-carbohydrazide derivatives as novel xanthine oxidase inhibitors, Bioorganic & medicinal chemistry, 27 (2019) 1818-1823.

[26] S. Sharma, K. Sharma, R. Ojha, D. Kumar, G. Singh, K. Nepali, P.M. Bedi, Microwave assisted synthesis of naphthopyrans catalysed by silica supported fluoroboric acid as a new class of non purine xanthine oxidase inhibitors, Bioorganic & medicinal chemistry letters, 24 (2014) 495-500.

[27] H. Singh, S. Sharma, R. Ojha, M.K. Gupta, K. Nepali, P.M. Bedi, Synthesis and evaluation of naphthoflavones as a new class of non purine xanthine oxidase inhibitors, Bioorganic & medicinal chemistry letters, 24 (2014) 4192-4197.

[28] T. Zhang, Y. Lv, Y. Lei, D. Liu, Y. Feng, J. Zhao, S. Chen, F. Meng, S. Wang, Design, synthesis and biological evaluation of 1-hydroxy-2-phenyl-4-pyridyl-1*H*-imidazole derivatives as xanthine oxidase inhibitors, European journal of medicinal chemistry, 146 (2018) 668-677.

[29] J. J. Baldwin, P. A. Kasinger, F. C. Novello, J. M. Sprague, 4-Trifluoromethylimidazoles and 5-(4-pyridyl)-1, 2, 4-triazoles, new classes of xanthine oxidase inhibitors, Journal of medicinal chemistry, 18 (1975) 895-900.

[30] M.R. Ali, S. Kumar, O. Afzal, N. Shalmali, M. Sharma, S. Bawa, Development of 2-(Substituted Benzylamino)-4-Methyl-1, 3-Thiazole-5-Carboxylic Acid Derivatives as Xanthine Oxidase Inhibitors and Free Radical Scavengers, Chemical Biology & Drug Design, 87 (2016) 508-516.

[31] T.J. Zhang, Q.X. Wu, S.Y. Li, L. Wang, Q. Sun, Y. Zhang, F.H. Meng, H. Gao, Synthesis and evaluation of 1-phenyl-1*H*-1,2,3-triazole-4-carboxylic acid derivatives as xanthine oxidase inhibitors, Bioorganic & medicinal chemistry letters, 27 (2017) 3812-3816.

[32] T. J. Zhang, S. Y. Li, Y. Zhang, Q. X. Wu, F.H. Meng, Design, synthesis, and biological evaluation of 5-[4-(pyridin-4-yl)-1*H*-1,2,3-triazol-1-yl] benzonitrile derivatives as xanthine oxidase inhibitors, Chemical Biology & Drug Design, 91 (2018) 526-533.

[33] S. Shukla, D. Kumar, R. Ojha, M.K. Gupta, K. Nepali, P.M.S. Bedi, 4,6-Diaryl/heteroarylpyrimidin-2(1*H*)-ones as a New Class of Xanthine Oxidase Inhibitors, Archiv der Pharmazie, 347 (2014) 486-495.

[34] C. B-Rao, A. Kulkarni-Almeida, K.V. Katkar, S. Khanna, U. Ghosh, A. Keche, P. Shah, A. Srivastava, V. Korde, K.V.S. Nemmani, N.J. Deshmukh, A. Dixit, M.K. Brahma, U. Bahirat, L. Doshi, R. Sharma, H. Sivaramakrishnan,

Identification of novel isocytosine derivatives as xanthine oxidase inhibitors from a set of virtual screening hits, Bioorganic & medicinal chemistry, 20 (2012) 2930-2939.

[35] F. H. Messerli, M. Burnier, Cardiovascular disease and uric acid: is the not-so-innocent bystander becoming a true culprit and does the US black box warning for febuxostat indicate that not all uric acid lowering is beneficial?[J]. European heart journal, 2019, 40(22): 1787-1789.

[36] P. Zhan, Y. Itoh, T. Suzuki, X. Liu, Strategies for the Discovery of Target-Specific or Isoform-Selective Modulators, Journal of Medicinal Chemistry, 58 (2015) 7611-7633.

[37] M. Huang, Y. Shao, J. Hou, W. Cui, B. Liang, Y. Huang, Z. Li, Y. Wu, X. Zhu, P. Liu, Y. Wan, H. Ke, H.B. Luo, Structural Asymmetry of Phosphodiesterase-9A and a Unique Pocket for Selective Binding of a Potent Enantiomeric Inhibitor, Molecular Pharmacology, 88 (2015) 836-845.

[38] D. Duchêne, E. Colombo, A. Désilets, P.-L. Boudreault, R. Leduc, E. Marsault, R. Najmanovich, Analysis of Subpocket Selectivity and Identification of Potent Selective Inhibitors for Matriptase and Matriptase-2, Journal of Medicinal Chemistry, 57 (2014) 10198-10204.

[39] M. Bartolowits, V.J. Davisson, Considerations of Protein Subpockets in Fragment-Based Drug Design, Chemical Biology & Drug Design, 87 (2016) 5-20.

[40] A.R. Blaazer, A.K. Singh, E. de Heuvel, E. Edink, K.M. Orrling, J.J.N. Veerman, T. van den Bergh, C. Jansen, E. Balasubramaniam, W.J. Mooij, H. Custers, M. Sijm, D.N.A. Tagoe, T.D. Kalejaiye, J.C. Munday, H. Tenor, A. Matheeussen, M. Wijtmans, M. Siderius, C. de Graaf, L. Maes, H.P. de Koning, D.S. Bailey, G.J. Sterk, I.J.P. de Esch, D.G. Brown, R. Leurs, Targeting a Subpocket in Trypanosoma brucei Phosphodiesterase B1 (TbrPDEB1) Enables the Structure-Based Discovery of Selective Inhibitors with Trypanocidal Activity, J Med Chem, 61 (2018) 3870-3888.

[41] L. Rahbarnia, S. Farajnia, H. Babaei, J. Majidi, K. Veisi, S. Khosroshahi, A. Tanomand, Development of a Novel Human scFv Against EGFR L2 Domain by Phage Display Technology, Current Pharmaceutical Design, 23 (2017) 2009-2014.

[42] K.A.K. Musa, V.R. Palwai, L.A. Eriksson, New nonsteroidal anti-inflammatory molecules with reduced photodegradation side effects and enhanced COX-2 selectivity, International Journal of Quantum Chemistry, 111 (2011) 1184-1195.

[43] E.A. Popova, A.V. Protas, R.E. Trifonov, Tetrazole Derivatives as Promising Anticancer Agents, Anti-cancer agents in medicinal chemistry, 17 (2018) 1856-1868.

[44] M.A. Malik, M.Y. Wani, S.A. Al-Thabaiti, R.A. Shiekh, Tetrazoles as carboxylic acid isosteres: chemistry and biology, Journal of Inclusion Phenomena and Macrocyclic Chemistry, 78 (2013) 15-37.

[45] V.A. Ostrovskii, E.A. Popova, R. E. Trifonov, Developments in tetrazole chemistry (2009–16), Advances in

Heterocyclic Chemistry, 123 (2017) 1-62.

[46] H. Qi, C. Kou, Y.J. Qi, B.H. Tang, Y.E. Wu, F. Jin, X.J. Luo, Y.H. Shen, Y.J. Guo, X. Qi, Y.C. Wang, Q. Dong, X.K. Chen, H.Y. Shi, Y. Zheng, W. Zhao, A.D. Shen, Population pharmacokinetics and dosing optimization of latamoxef in neonates and young infants, International journal of antimicrobial agents, 53 (2019) 347-351.

[47] Y. Zhao, J. Cao, A. Melamed, M. Worley, A. Gockley, D. Jones, H.T. Nia, Y. Zhang, T. Stylianopoulos, A.S. Kumar, F. Mpekris, M. Datta, Y. Sun, L. Wu, X. Gao, O. Yeku, M.G. Del Carmen, D.R. Spriggs, R.K. Jain, L. Xu, Losartan treatment enhances chemotherapy efficacy and reduces ascites in ovarian cancer models by normalizing the tumor stroma, Proceedings of the National Academy of Sciences of the United States of America, 116 (2019) 2210-2219.

[48] P. Vandenberghe, M. Delvaux, P. Hagué, C. Erneux, J. M. Vanderwinden, Potentiation of imatinib by cilostazol in sensitive and resistant gastrointestinal stromal tumor cell lines involves YAP inhibition, Oncotarget, 10 (2019) 1798-1811.

[49] C. Gao, L. Chang, Z. Xu, X.F. Yan, C. Ding, F. Zhao, X. Wu, L.S. Feng, Recent advances of tetrazole derivatives as potential anti-tubercular and anti-malarial agents, European journal of medicinal chemistry, 163 (2019) 404-412.

[50] J.W. De Schutter, J.P. Morrison, M.J. Morrison, A. Ciulli, B. Imperiali, Targeting Bacillosamine Biosynthesis in Bacterial Pathogens: Development of Inhibitors to a Bacterial Amino-Sugar Acetyltransferase from Campylobacter jejuni, J Med Chem, 60 (2017) 2099-2118.

[51] A. Khandelwal, V.M. Crowley, B.S.J. Blagg, Resorcinol-Based Grp94-Selective Inhibitors, ACS medicinal chemistry letters, 8 (2017) 1013-1018.

[52] D.K. Tosh, S. Paoletta, F. Deflorian, K. Phan, S.M. Moss, Z.G. Gao, X. Jiang, K.A. Jacobson, Structural sweet spot for A1 adenosine receptor activation by truncated (N)-methanocarba nucleosides: receptor docking and potent anticonvulsant activity, J Med Chem, 55 (2012) 8075-8090.

[53] R. Kaur, P. Kaur, S. Sharma, G. Singh, S. Mehndiratta, P. M. S, Bedi, K. Nepali, Anti-cancer pyrimidines in diverse scaffolds: a review of patent literature, Recent patents on anti-cancer drug discovery, 10 (2015) 23-71.

[54] J.R. Corte, T. Fang, D.J. Pinto, M.J. Orwat, A.R. Rendina, J.M. Luettgen, K.A. Rossi, A. Wei, V. Ramamurthy, J.E. Myers, Jr., S. Sheriff, R. Narayanan, T.W. Harper, J.J. Zheng, Y.X. Li, D.A. Seiffert, R.R. Wexler, M.L. Quan, Orally bioavailable pyridine and pyrimidine-based Factor XIa inhibitors: Discovery of the methyl N-phenyl carbamate P2 prime group, Bioorganic & medicinal chemistry, 24 (2016) 2257-2272.

[55] A.N. Vorobiov, P.N. Gaponik, P.T. Petrov, O.A. Ivashkevich, One-Pot Syntheses of 5-Amino-1-aryltetrazole Derivatives, Synthesis, 08 (2006) 1307-1312.

[56] S. Salerno, A.M. Marini, G. Fornaciari, F. Simorini, C. La Motta, S. Taliani, S. Sartini, F. Da Settimo, A.N.

Garcia-Argaez, O. Gia, S. Cosconati, E. Novellino, P. D'Ocon, A. Fioravanti, P. Orlandi, G. Bocci, L. Dalla Via, Investigation of new 2-aryl substituted Benzothiopyrano[4,3-*d*]pyrimidines as kinase inhibitors targeting vascular endothelial growth factor receptor 2, European journal of medicinal chemistry, 103 (2015) 29-43.

[57] B. Purushothaman, P. Arumugam, G. Kulsi, J.M. Song, Design, synthesis, and biological evaluation of novel catecholopyrimidine based PDE4 inhibitor for the treatment of atopic dermatitis, European journal of medicinal chemistry, 145 (2018) 673-690.

[58] Z. Xie, X. Luo, Z. Zou, X. Zhang, F. Huang, R. Li, S. Liao, Y. Liu, Synthesis and evaluation of hydroxychalcones as multifunctional non-purine xanthine oxidase inhibitors for the treatment of hyperuricemia, Bioorganic & medicinal chemistry letters, 27 (2017) 3602-3606.

[59] Guideline, Performance-Based Test. "OECD guideline for the testing of chemicals." *The Hershberger* 601 (2001): 858.

[60] Glide, Schrodinger, LLC, New York, NY, 2016.

[61] M.R. Ali, S. Kumar, O. Afzal, N. Shalmali, W. Ali, M. Sharma, S. Bawa, 2-Benzamido-4-methylthiazole-5-carboxylic Acid Derivatives as Potential Xanthine Oxidase Inhibitors and Free Radical Scavengers, Archiv der Pharmazie, 350 (2017) 1600313.

[62] Visualizer A D S. Version 4. 5[J]. Softw. Vis. Anal. Protein Struct, 2017.

[63] The PyMOL Molecular Graphics System, version 1.5.0.3; Schrödinger, LLC: New York.

[64] L. Hongyan, W. Suling, Z. Weina, Z. Yajie, R. Jie, Antihyperuricemic effect of liquiritigenin in potassium oxonate-induced hyperuricemic rats, Biomedicine & Pharmacotherapy, 84 (2016) 1930-1936.

[65] M.T.T. Nguyen, S. Awale, Y. Tezuka, L. Shi, S.F.H. Zaidi, J. Ueda, Q.L. Tran, Y. Murakami, K. Matsumoto, S. Kadota, Hypouricemic effects of acacetin and 4, 5-*o*-dicaffeoylquinic acid methyl ester on serum uric acid levels in potassium oxonate-pretreated rats, Biological and Pharmaceutical Bulletin, 28 (2005) 2231-2234.

[66] N. Liu, Y. Wang, M. Yang, W. Bian, L. Zeng, S. Yin, Z. Xiong, Y. Hu, S. Wang, B. Meng, J. Sun, X. Yang, A new rice-derived short peptide potently alleviated hyperuricemia induced by potassium oxonate in rats, Journal of agricultural and food chemistry, 67 (2019) 220-228.

Highlights

• Analysis of the high-resolution structure of XO with febuxostat identified the existance of a subpocket formed by the residues Leu648, Asn768, Lys771, Leu1014 and Pro1076.

•2-[4-alkoxy-3-(*1H*-tetrazol-1-yl)phenyl]-6-oxo-1,6-dihydropyrimidine-5-carboxylic acid derivatives were synthesized.

• The inhibitory potency of these compounds against XO *in vitro* was evaluated and compound **8u** showed a promising XO inhibitory potency with an IC_{50} value of 0.0288 μM.

• The structure–activity relationships of the synthesized compounds were summarized.

• Molecular modeling studies, steady-state kinetic analysis, acute oral toxicity study and a hyperuricemia rat model were performed.